REPORT DOCUMENTATION PAGE

AFRL-SR-BL-TR-01-

0031

1. AGENCY USE ONLY *(Leave blank)*	2. REPORT DATE	3. REPT
		FINAL REPORT 09-01-97 TO 09-01-98

4. TITLE AND SUBTITLE
EFFECT OF MICROSTRUCTURE ON THE THERMOMECHANICAL PROPERTIES OF SIC FIBERS

5. FUNDING NUMBERS
F49620-97-1-0095

6. AUTHOR(S)
M. D. SACKS
J. H. SIMMONS

7. PERFORMING ORGANIZATION NAME(S) AND ADDRESS(ES)
DEPARTMENT OF METERIALS SCIENCE AND ENGINEERING
UNIVERSITY OF FLORIDA
GAINESVILLE, FL 32611

8. PERFORMING ORGANIZATION REPORT NUMBER

9. SPONSORING/MONITORING AGENCY NAME(S) AND ADDRESS(ES)
AIR FORCE OFFICE OF SCIENTIFIC RESEARCH
801 N. RANDOLPH STREET, ROOM 732
ARLINGTON, VA 22203

10. SPONSORING/MONITORING AGENCY REPORT NUMBER

11. SUPPLEMENTARY NOTES

12a. DISTRIBUTION AVAILABILITY STATEMENT

Approved for public release;
distribution unlimited.

13. ABSTRACT *(Maximum 200 words)*

Polymer-derived SiC-based fibers with fine-diameter (10-15 mm) and high strength (3 GPa) were prepared with carbon-rich and near-stoichiometric compositions. Fiber tensile strengths were determined after heat treatments at temperatures up to 1950oC in non-oxidizing atmospheres and up to 1250oC in air. The creep resistance of fibers was assessed using bend stress relaxation (BSR) measurements. Fibers showed excellent strength retention after heat treatments in non-oxidiziing atmospheres at temperatures up to 1700oC for the carbon-rich fibers and up to 1950oC for the near-stoichiometric fibers. The near-stoichiometric fibers also showed considerably better strength retention after heat treatments in air. Creep resistance of the as-fabricated fibers was greatly improved by high-temperature heat treatments. Heat-treated near-stoichiometric fibers could be prepared with 3 GPa tensile strengths and BSR creep behavior which was significantly better than that reported for i-Nicalon TM Type S fibers. It was also shown that the near-stoichiometric fibers could be coated with hexagonal BN using an in-situ processing method.

14. SUBJECT TERMS	15. NUMBER OF PAGES
	64
	16. PRICE CODE

17. SECURITY CLASSIFICATION OF REPORT	18. SECURITY CLASSIFICATION OF THIS PAGE	19. SECURITY CLASSIFICATION OF ABSTRACT	20. LIMITATION OF ABSTRACT
UNCLASSIFIED	UNCLASSIFIED	UNCLASSIFIED	

EFFECT OF MICROSTRUCTURE ON THE THERMOMECHANICAL PROPERTIES OF SIC FIBERS

Progress Report (09/01/97 - 9/01/98)

AFOSR Grant No. F49620-97-1-0095

Submitted to:

Dr. Alexander Pechenik
Air Force Office of Scientific Research
110 Duncan Avenue, Suite B115
Bolling AFB DC 20332-8080

Submitted by:

M.D. Sacks and J.H. Simmons
Dept. of Materials Science and Engineering
University of Florida
Gainesville, FL 32611

OUTLINE

1.0 EXECUTIVE SUMMARY

Polymer-derived SiC-based fibers with fine-diameter (~10-15 μm) and high strength (~3 GPa) were prepared with carbon-rich and near-stoichiometric compositions. Fiber tensile strengths were determined after heat treatments at temperatures up to 1950°C in non-oxidizing atmospheres and up to 1250°C in air. The creep resistance of fibers was assessed using bend stress relaxation (BSR) measurements. Fibers showed excellent strength retention after heat treatments in non-oxidizing atmospheres at temperatures up to 1700°C for the carbon-rich fibers and up to 1950°C for the near-stoichiometric fibers. The near-stoichiometric fibers also showed considerably better strength retention after heat treatments in air. Creep resistance of the as-fabricated fibers was greatly improved by high-temperature heat treatments. Heat-treated near-stoichiometric fibers could be prepared with ~3 GPa tensile strengths and BSR creep behavior which was significantly better than that reported for Hi-Nicalon™ Type S fibers. It was also shown that the near-stoichiometric fibers could be coated with hexagonal BN using an in-situ processing method.

Modeling and simulation studies were conducted in conjunction with the experimental fiber processing and characterization efforts in order to develop an understanding of underlying processes that control high temperature creep and grain growth in SiC fibers. The modeling studies have developed a creep equation for 2-dimensional creep due to intragranular diffusion. Simulations were conducted using a novel method of Hybrid Monte Carlo to determine the relative diffusion coefficients of Si and C in SiC grains. Preliminary results show promise in determining the differences in diffusion coefficients between the two species.

2.0 INTRODUCTION

There has been considerable interest in recent years in producing SiC-based fibers with improved thermomechanical properties. Much of the effort in this area has been directed toward fabrication of fine-diameter, high-strength, polymer-derived fibers which have low oxygen content.[1-7] The development of such fibers with both carbon-rich and near-stoichiometric compositions have been reported by several research groups, including those at Nippon Carbon Co. (Hi-Nicalon™ and Hi-Nicalon™ Type S fibers)[1-3], Dow Corning Co. (Sylramic™ fibers)[4,5], and the University of Florida (UF and UF-HM fibers).[6,7] All of these fibers show improved thermochemical stability and thermomechanical properties compared to fibers which contain large amounts of oxygen, such as Nicalon™ and Tyranno™ fibers. The latter fibers undergo extensive carbothermal reduction reactions at elevated temperatures which degrade fiber properties as a result of the formation of porosity, large grains, and other flaws. In contrast, such reactions are substantially reduced or avoided in the low-oxygen-content fibers. However, characterization of the thermo-mechanical properties of these fibers is still relatively limited and the effects of microstructural factors on properties is not clearly understood. Of particular importance is the need to develop an improved understanding of the factors which control the strength retention and the creep behavior under various environmental conditions (e.g., oxidizing and non-oxidizing atmospheres). Creep becomes an important deformation mechanism at temperatures which are substantially lower than thermal decomposition or melting temperatures. Hence, creep may determine the limiting temperature for which SiC-fiber based CMC's can be used in structural applications requiring long-term stability at elevated temperature.

The present research program combines (i) experimental studies to produce fibers with controlled structures which are being used to establish microstructure-thermomechanical property relationships and (ii) computer modeling and simulation studies to understand the atomistic mechanisms underlying high temperature behavior (such as creep and strength retention) in order to both analyze the results of experiments and guide the development of new structures for improved properties.

3.0 RESULTS AND DISCUSSION

3.1 Experimental Studies

The experimental results are summarized below. Additional details are provided in two papers which are attached in the Appendix.

SiC-based fibers were fabricated with varying microstructural characteristics, including the Si/C ratio, grain size, and dopant type and concentration. The fiber microstructure were characterized using techniques such as conventional and high resolution transmission electron microscopy (HRTEM), X-ray and electron diffraction, and bulk and microchemical compositional analyses. In the initial work, the tensile strength and creep resistance of carbon-rich UF fibers and near-stoichiometric UF-HM fibers were evaluated before and after heat treatments at temperatures up to 1950°C. The creep resistance was assessed using the bend stress relaxation (BSR) method of Morscher and DiCarlo.[8] In this method, stress relaxation values (designated as "M" values) are determined based on the extent of permanent deformation that occurs when fibers are heat treated under an applied bending load. Fibers are considered more thermally stable against creep as the M values increase from 0 to 1.

SiC-based fibers with carbon-rich (UF fibers) composition and near-stoichiometric composition (UF-HM fibers) were fabricated. The as-fabricated UF fibers had an average composition (determined using electron microprobe analysis, EMA) of ~60.5 wt% Si/~39.5 wt% C. Hence, these fibers were highly carbon-rich relative to stoichiometric SiC (~70 wt% Si/~30 wt% C). Oxygen was present in the fibers as an impurity picked up during various stages of processing.[6] The concentrations usually did not exceed 1.5 wt% and were more typically in the range of ~0.5-1.0 wt%. The phases present in the UF fibers were β-SiC and XRD-amorphous carbon. TEM and XRD line-broadening measurements indicated that the β-SiC crystallite sizes in the as-fabricated fibers were less than 5 nm. The fibers had an average tensile strength of ~3.2 GPa and diameters were typically ~10-15 μm. Previous fractography studies on similar fibers indicated that the strength-controlling flaw sizes were mostly in the range of ~0.2-0.3 μm.[9] This corresponds closely to the smallest pore sizes of the filters (nominal sizes were 0.1-0.2 μm) that were used to prepare the spinning solutions for fiber fabrication. Hence, it is believed that the tensile strength of the UF fibers is controlled primarily by processing-related particulates (i.e., impurity particles, polymer "microgel" particles, etc.).

The near-stoichiometric UF-HM fibers had an average composition (determined using EMA) of ~68.5 wt% Si/~31.5 wt% C which indicates that the fibers usually contained a small amount of excess carbon. X-ray and electron diffraction analyses of the UF-HM fibers showed that β-SiC was the primary phase in the fibers, although traces of the alpha phase were observed in some fibers. The SiC grain sizes in the as-fabricated samples were generally in the range of ~0.05 - 0.3 μm, although grains as large as ~0.5-1.0 μm were occasionally observed. Residual carbon was not detected by a standard XRD powder diffraction method, but was observed by TEM. HRTEM analysis showed the stacked hexagonal structural units with interplanar spacing of 0.34 nm that are associated with graphitic carbon. EMA analysis for oxygen and nitrogen showed that concentrations were less than the resolution limit for the technique (typically $\leq$0.2 wt%). Boron was used as a

ing aid and was typically present in the as-fabricated fiber at concentrations of ~1 wt%. The ensile strength was ~2.8 GPa and the fibers diameters were typically in the range of ~10-14 he tensile strengths of the as-fabricated UF-HM fibers were probably controlled primarily by grains at the fiber surface. (Fracture was generally initiated at the surface, but it was difficult ntify the specific flaws responsible for failure.)

ure 1 shows room temperature tensile strengths for UF and UF-HM fibers after heat treatments argon for 1 h at temperatures in the range of 1400-1950°C. The near-stoichiometric UF-HM fibers retained most of their original strength through heat treatments up to 1800°C and then the strength gradually decreased with heat treatments at higher temperatures (up to 1950°C). The UF fibers showed no loss in strength with heat treatments up to 1700°C and then showed sharper decreases in strength (compared to the UF-HM fibers) with further heat treatments up to 1900°C. Despite these differences, both the UF fibers and the UF-HM fibers show greater retention of their original strengths after high temperature (e.g., $\geq$1600°C) heat treatments in argon compared to the strength retention reported for carbon-rich Hi-Nicalon™ fibers and near-stoichiometric Hi-Nicalon™ Type S fibers, respectively.[2,10]

As noted earlier, it is believed that the strength-controlling flaws for the as-prepared UF-HM fibers are larger grains at the fiber surfaces. Therefore, the gradual decrease in tensile strength in the UF-HM fibers after heat treatment in argon at higher temperatures is attributed to grain growth. A small increase in the grain sizes was confirmed by TEM observations on a 1950°C heat-treated sample.[11]

It is not clear why the UF fibers decreased in tensile strength at lower heat treatment temperature (and decreased more sharply with increasing temperature) compared to the UF-HM fibers. One possible explanation is that carbothermal reduction reactions occurred due to the small amount of residual oxygen in the fibers, thereby creating strength-degrading flaws. However, supporting evidence for this explanation is lacking. Scanning electron microscope (SEM) observations of the fibers (including the fracture surfaces) did not reveal the development of any obvious flaws, such as large pores or grains, which would account for the rapid decrease in strength with heat treatments above 1700°C. In addition, TEM observations showed that the grain sizes remained much smaller than those observed in the UF-HM fibers. Figure 2 shows TEM micrographs for a UF fiber heat treated for 1 h at 1900°C (in argon) and a UF-HM fiber heat treated for 0.2 h at 1840°C (in argon), respectively. Despite heat treatment at the higher temperature and longer time, the UF fibers have a considerably smaller average grain size compared to the UF-HM fibers. (The relatively slow grain growth in the UF fibers can be attributed to the much larger amount of excess carbon. This is expected to inhibit the Si diffusional transport that is required for SiC grain coarsening.)

Another possible explanation for the more rapid decay in strength of the UF fibers with heat treatment is the presence of residual tensile stresses at the fiber surface. Such stress might arise due to the mismatch in thermal expansion coefficients between SiC and C. These stresses could become more severe as the SiC/C structure coarsens during heat treatment at higher temperatures. (In addition to growth of the β-SiC grains, the carbon regions grow into larger and more highly ordered domains when PCS-derived carbon-rich SiC fibers are heat treated at temperatures above the original fabrication temperature.[10,12] The growth of the graphitic carbon regions also has significance because graphite has a very large difference in the thermal expansion coefficients for the directions parallel and normal to the hexagonal basal planes.)

Figure 1

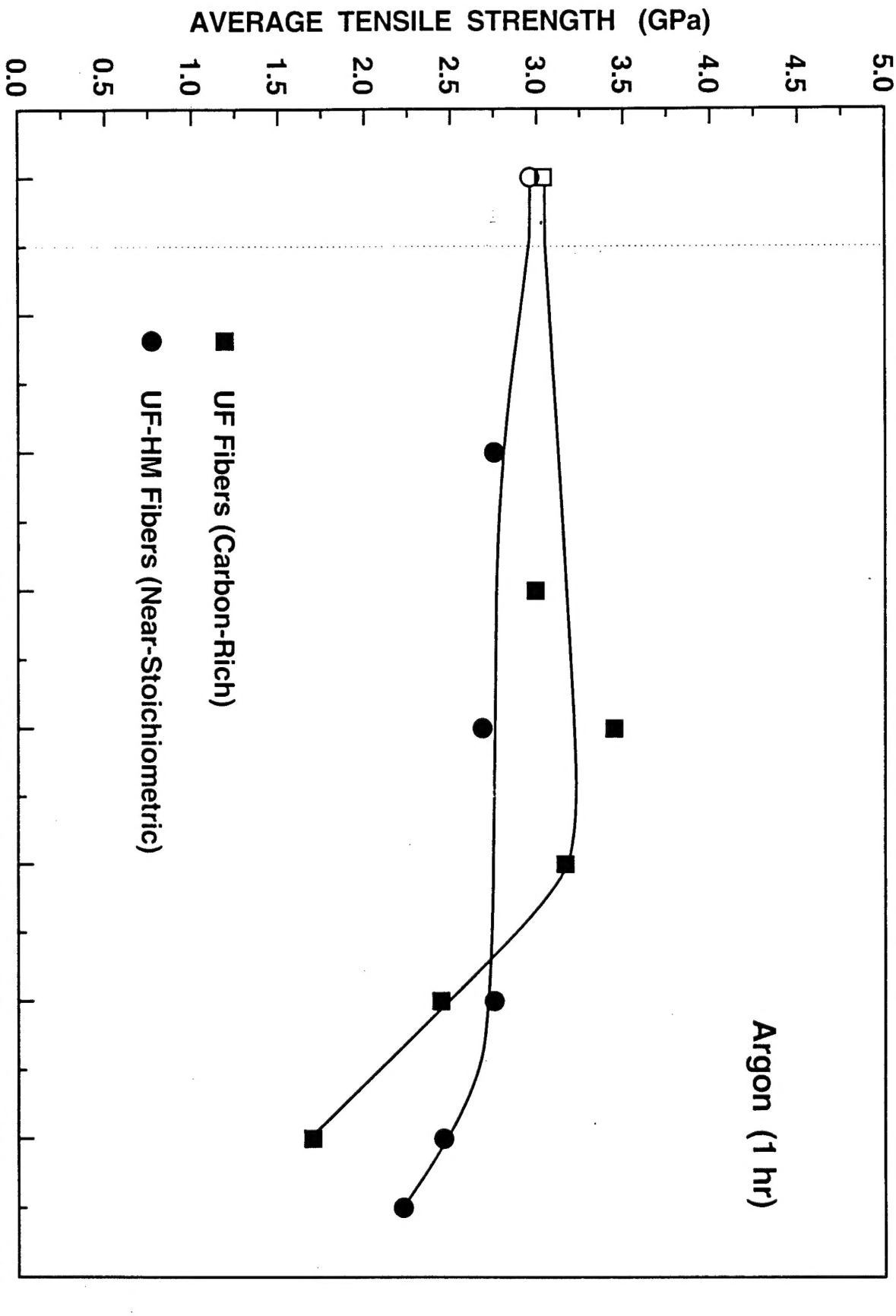
AVERAGE TENSILE STRENGTH (GPa)
0.0
0.5
1.0
1.5
2.0
2.5
3.0
3.5
4.0
4.5
5.0
Initial
1300
1400
1500
1600
1700
1800
1900
2000
HEAT TREATMENT TEMPERATURE (°C)
Argon (1 hr)
UF Fibers (Carbon-Rich)
UF-HM Fibers (Near-Stoichiometric)

Figure 2

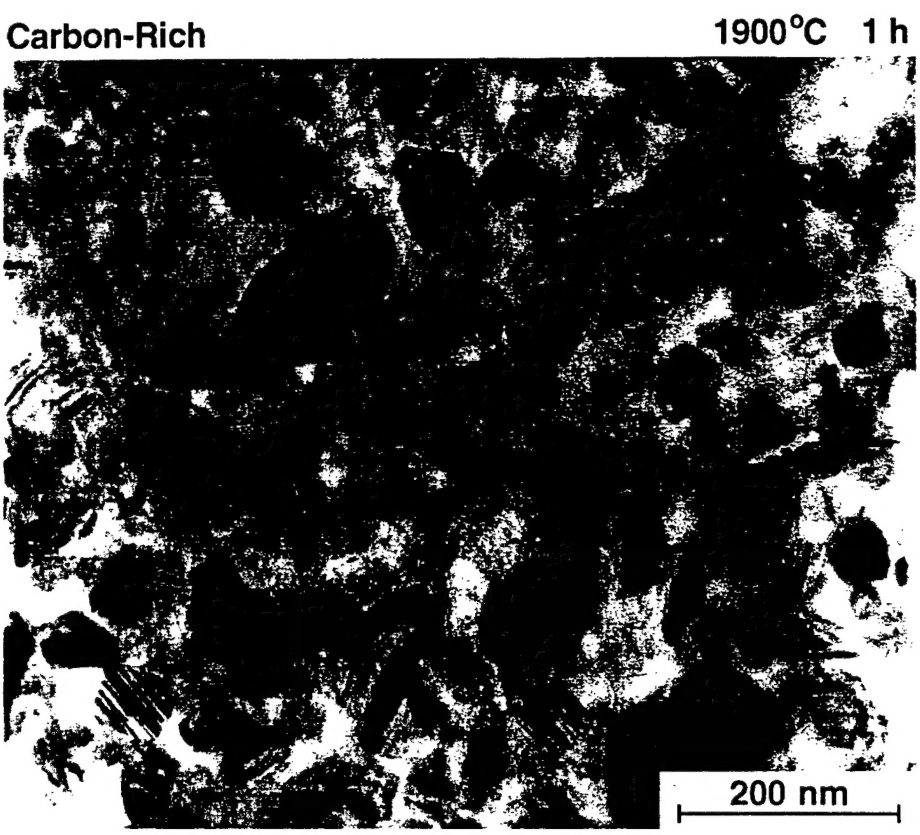
Carbon-Rich
1900°C 1 h
200 nm

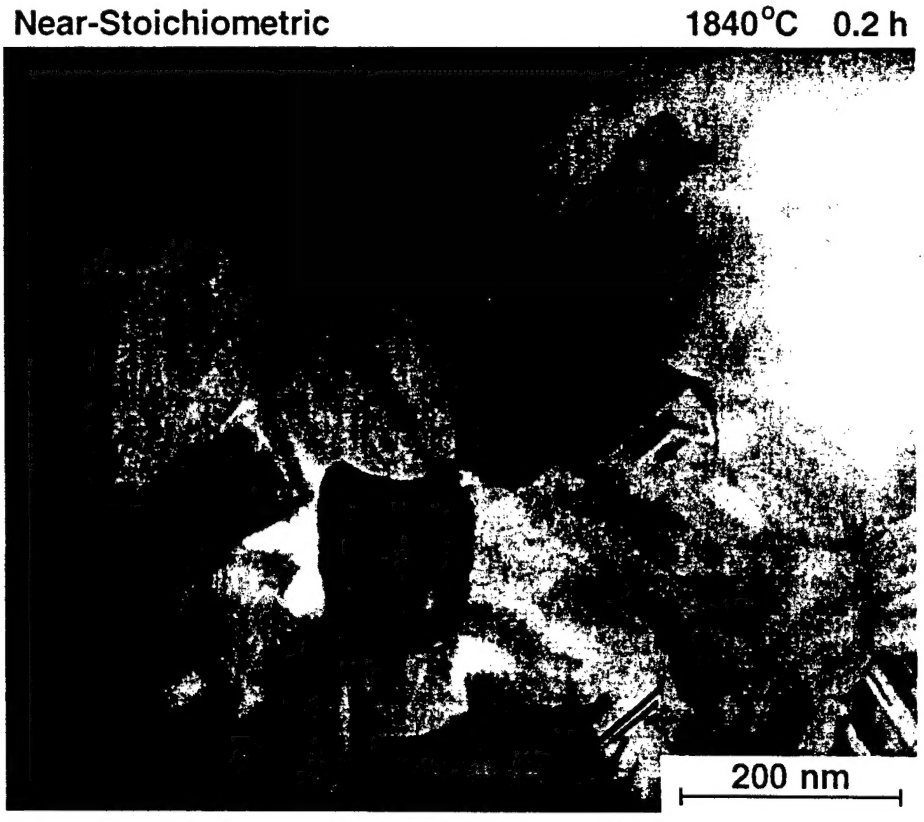
Near-Stoichiometric
1840°C 0.2 h
200 nm

The excellent strength retention of the UF and UF-HM fibers after high temperature heat treatments in argon (e.g., compared to fibers such as Hi-Nicalon™ and Hi-Nicalon™ Type S) offers the possibility for improved high-temperature strength retention in ceramic-matrix composites (CMC's) that are fabricated with such fibers. In addition, it is possible to prepare fibers with improved creep resistance, while still retaining high tensile strength. In regard to improving creep performance, it has been shown that Hi-Nicalon™ and Hi-Nicalon™ Type S fibers become more creep-resistant after annealing heat treatments above the original processing temperature.[3,13] (This may be attributed to the increased SiC grain sizes, as well as the more highly crystallized graphitic carbon regions in the fibers. Both microstructural changes would be expected to inhibit diffusion-controlled creep processes.) The same effect (i.e., improved creep resistance in annealed fibers) was observed in the present study for the UF and UF-HM fibers. Figure 3 shows plots of the bend stress relaxation ratios, M, as a function of the heat treatment temperature for as-pyrolyzed (1200°C) UF fibers and for UF fibers which were given heat treatments for 1 h (in argon) at 1700°C and 1900°C. As expected, substantial increases in M values were obtained for the heat-treated UF fibers. The 1700°C heat-treated UF fibers not only show greatly improved creep resistance (based on the BSR test results), but also retain high tensile strength.

Figure 3 also includes BSR data reported [3,14-16] for Hi-Nicalon™ and Hi-Nicalon™ Type S fibers. The Hi-Nicalon™ fibers have higher M values (for a given BSR test temperature) compared to the as-prepared UF fibers. This is attributed to a slightly higher initial processing temperature for the Hi-Nicalon™ fibers which, in turn, results in slightly coarser microstructures (including larger SiC crystallite sizes). The 1700°C heat-treated UF fibers have M values comparable or better (for a given BSR test temperature) than both Hi-Nicalon™ Type S fibers (Fig. 3) and as-fabricated UF-HM fibers (Fig. 4). This occurs despite the fact that the grain sizes are much larger for the latter two near-stoichiometric SiC fibers. This observation again suggests that Si diffusion is inhibited in SiC-based fibers with larger amounts of excess carbon. (This manifests itself not only in the slower coarsening of SiC grains, but also in the improved creep resistance of the fibers.)

Figure 4 shows that the creep resistance (as assessed by the BSR method) for the near-stoichiometric UF-HM fibers can also be improved by annealing heat treatments. In fact, the annealed UF-HM fibers show comparable BSR behavior to that reported [14-16] for much weaker, coarse-grained Carborundum fibers. (The latter fibers were prepared by sintering of SiC powders.[17] This resulted in fibers with considerably larger grain sizes, larger diameters, and rougher surfaces compared to typical polymer-derived SiC fibers. The coarser grain sizes result in fibers with excellent creep resistance, but relatively low tensile strength.) Takeda et al.[3] have also reported that annealing heat treatments can be used to improve the creep resistance of the Hi-Nicalon™ Type S fibers (as assessed by the BSR test). However, these fibers do not retain tensile strengths as high as the UF-HM fibers after the annealing heat treatments. It was possible to produce annealed UF-HM fibers which had a 1400°C BSR M value of ~ 0.9 and a 1600°C BSR M value of ~ 0.45, while still retaining tensile strengths of ~ 3 GPa in both cases. In contrast, 1400°C and 1600°C BSR M values of only ~ 0.6 and ~ 0.05, respectively, were possible in Hi-Nicalon™ Type S fibers which retained tensile strengths of ~ 3 GPa.

The improved creep resistance of the UF-HM fibers after the annealing treatment is attributed, at least in part, to increased grain sizes. It is also possible that boron removal from the bulk of the fiber (i.e., due to migration to the fiber surface) decreases SiC self-diffusion coefficients and thereby decreases the creep rate.

Figure 3

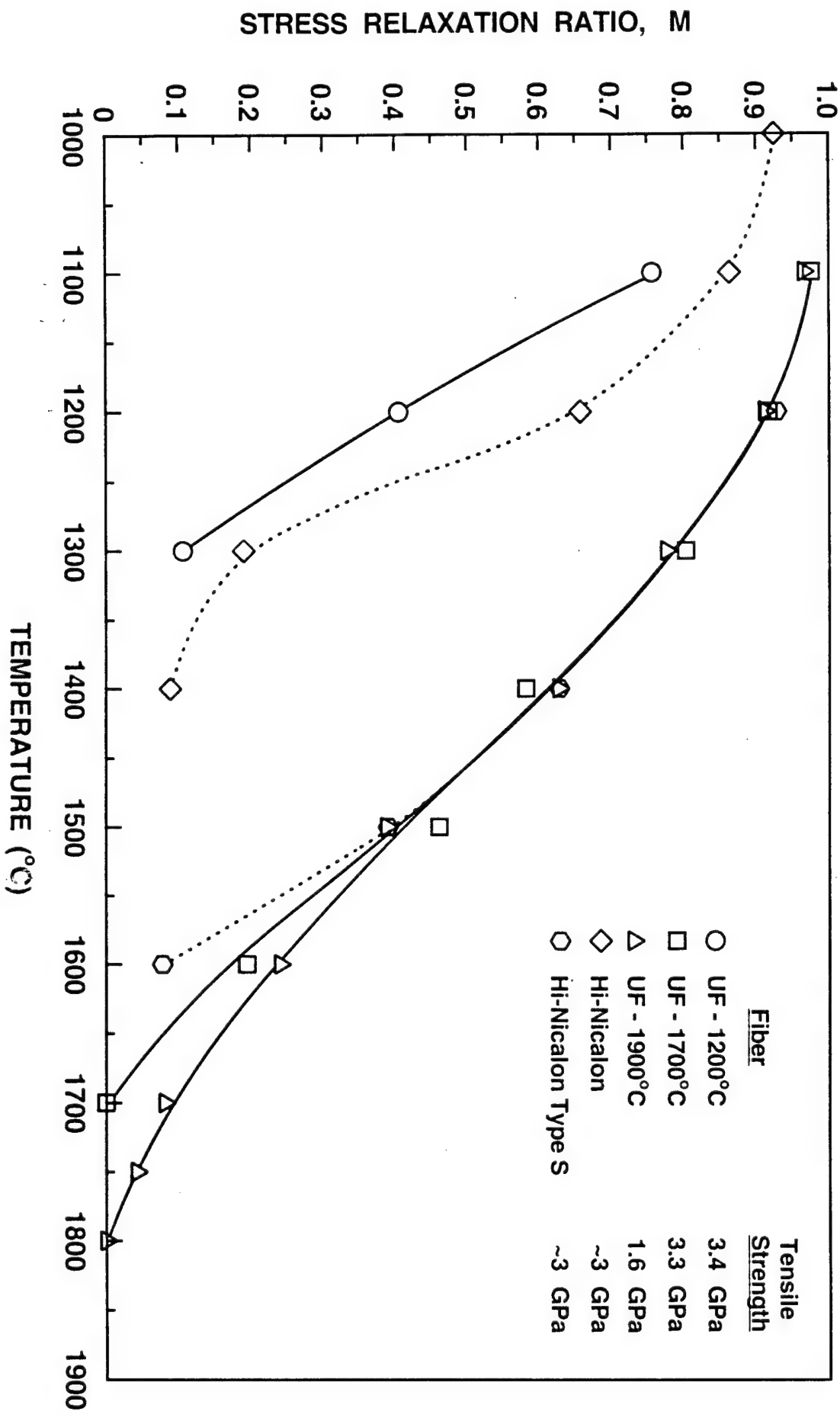
STRESS RELAXATION RATIO, M
1.0
0.9
0.8
0.7
0.6
0.5
0.4
0.3
0.2
0.1
0
1000
1100
1200
1300
1400
1500
1600
1700
1800
1900
TEMPERATURE (°C)
Fiber
Tensile Strength
UF - 1200°C 3.4 GPa
UF - 1700°C 3.3 GPa
UF - 1900°C 1.6 GPa
Hi-Nicalon ~3 GPa
Hi-Nicalon Type S ~3 GPa

Figure 4

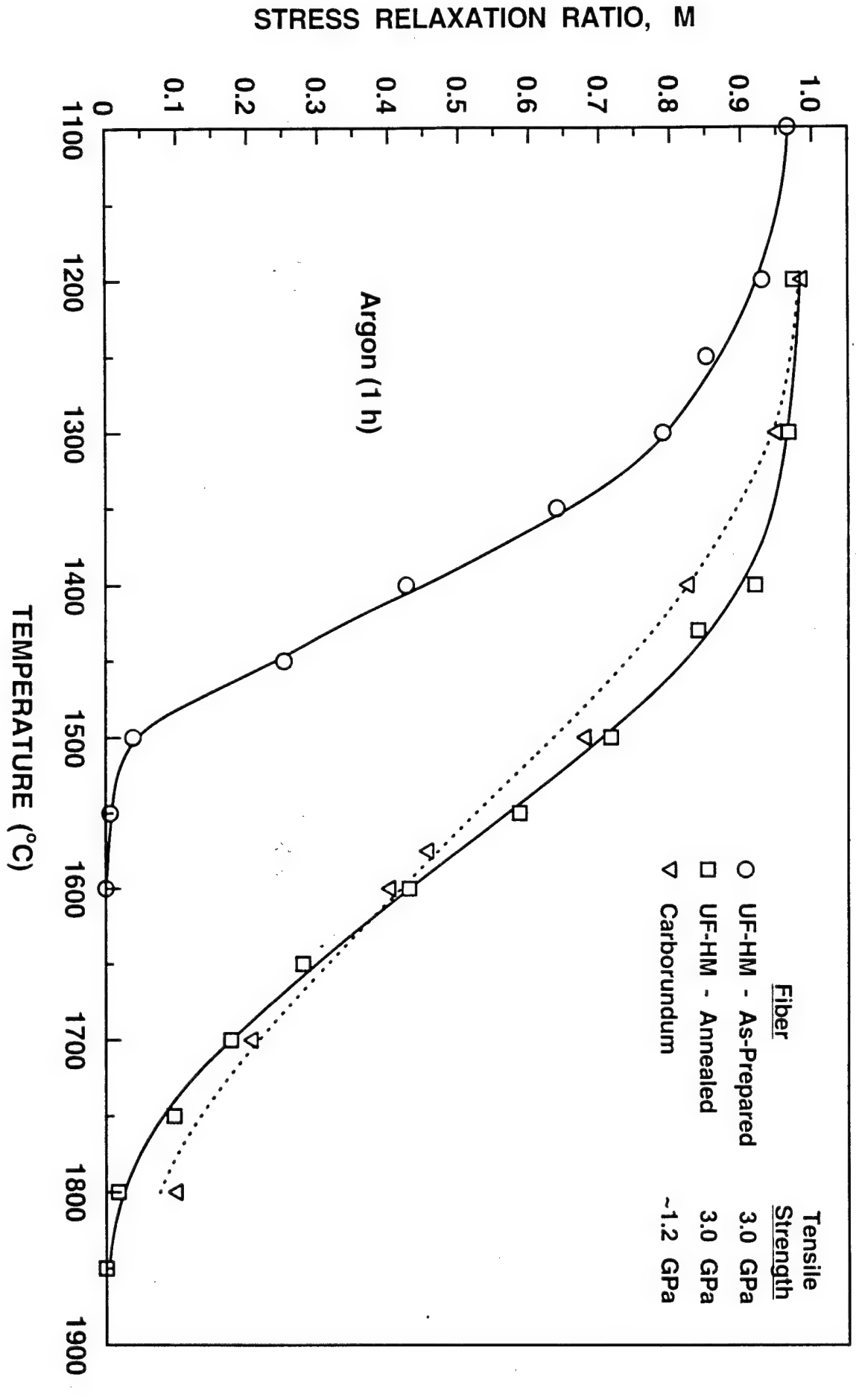
STRESS RELAXATION RATIO, M
1.0
0.9
0.8
0.7
0.6
0.5
0.4
0.3
0.2
0.1
0
1100
1200
1300
1400
1500
1600
1700
1800
1900
TEMPERATURE (°C)
Argon (1 h)
Fiber
Tensile Strength
UF-HM - As-Prepared 3.0 GPa
UF-HM - Annealed 3.0 GPa
Carborundum ~1.2 GPa

olyzed UF fibers and UF fibers heat treated in argon at 1650°C were subsequently given heat nts in air for 1 h at temperatures in the range of 500-1150°C. Figure 5 shows the room ature tensile strengths for these fibers after the air heat treatments. The decreases in strength ibuted to the formation of porosity (and possibly other flaws) resulting from the oxidative stion of the carbon phase in the fibers. The SiC/C fiber microstructure coarsens significantly the 1650°C argon annealing heat treatment and this evidently allows oxygen to react with the on phase more readily. The fiber strength begins to decrease in the range of only 500-600°C, e., at similar temperatures for which significant reaction occurs when bulk carbon is heat treated to air. The tensile strengths for the 1650°C fibers level off after the 900°C air heat treatment which apparently correlates with the removal of most of the excess carbon from the fiber. In contrast to these results, the oxidative removal of carbon from the as-pyrolyzed UF fibers occurs at considerably higher temperatures. Strength decreases are not observed until the air heat treatment temperature is greater than ~950°C. This is attributed to the development of thin siliceous surface layers during air heat treatment which would inhibit oxidative removal of the carbon at the lower temperatures.

Figure 6 shows the room temperature tensile strengths for as-sintered UF-HM fibers after they were heat treated in air for 1 h at temperatures in the range of 400-1250°C. The fibers show excellent strength retention under these heat treatment conditions. After the 1250°C heat treatment in air, it was observed that the individual fibers were beginning to stick together (i.e., presumably due to viscous flow of the silica surface layers). It is likely that surface damage was introduced when these fibers were separated for the tensile tests.

It was also shown that the near-stoichometric UF-HM fibers could be prepared with BN surface coatings by an in-situ process, as shown schematically illustrated in Fig. 7. Fibers were initially with boron dopant and then were heat treated in a nitrogen-containing atmosphere. BN forms by reaction of boron at the surface with nitrogen in the atmosphere. Typical BN coating thicknesses were ~0.1-0.2 μm, although it may be possible to increase the thickness by using SiC fibers with higher initial boron content. Electron diffraction analysis and the lattice spacing value (0.346 nm) determined by HRTEM showed that the layer was hexagonal BN. HRTEM also showed that the coating grows such that the hexagonal BN basal planes are oriented mostly perpendicular to the long axis of the fibers. The fibers prepared with the BN coatings retained high strength (~3 GPa) and excellent creep resistance.

Figure 5

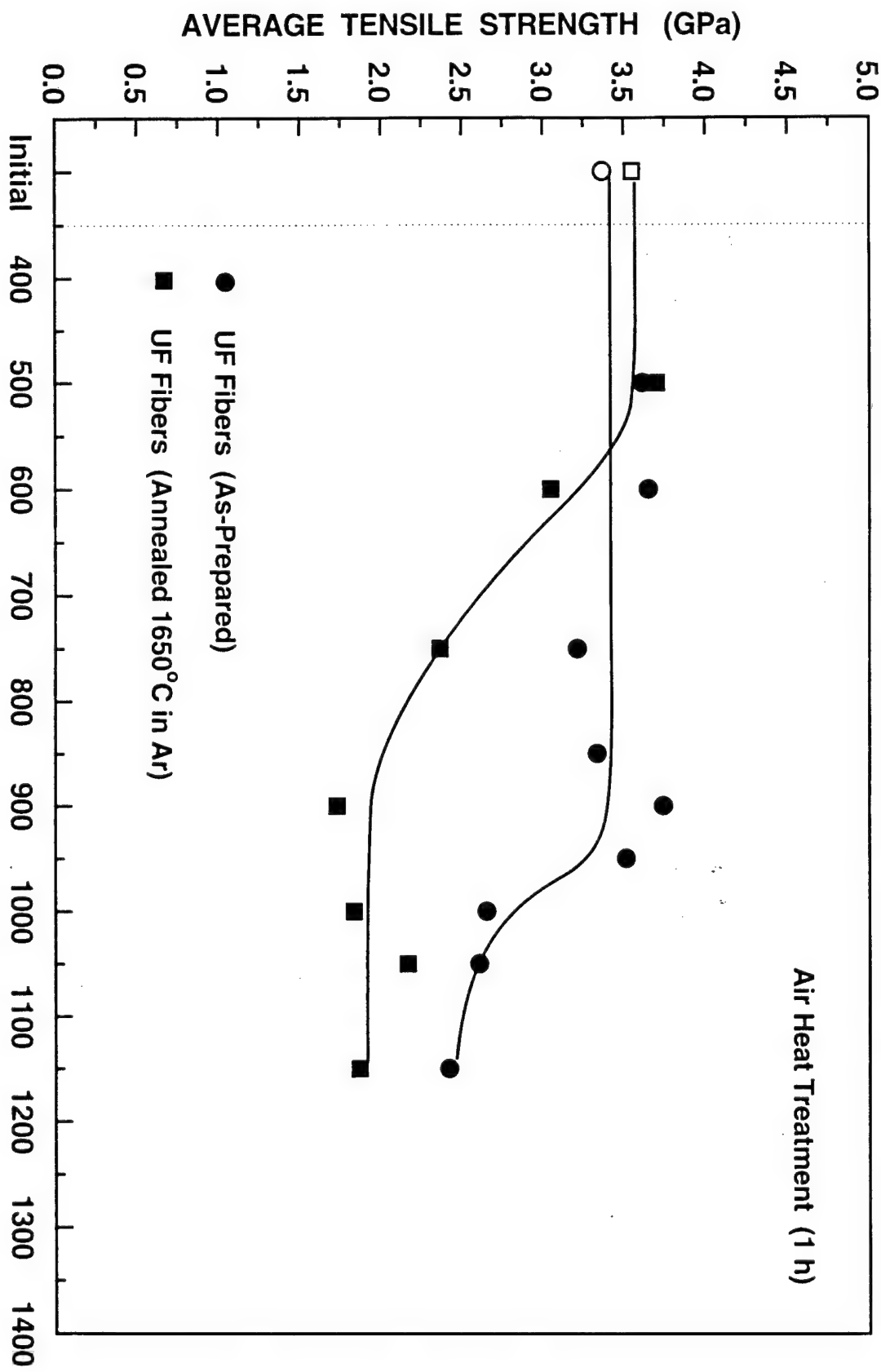
AVERAGE TENSILE STRENGTH (GPa)
0.0
0.5
1.0
1.5
2.0
2.5
3.0
3.5
4.0
4.5
5.0
Initial
400
500
600
700
800
900
1000
1100
1200
1300
1400
HEAT TREATMENT TEMPERATURE (°C)
Air Heat Treatment (1 h)
UF Fibers (As-Prepared)
UF Fibers (Annealed 1650°C in Ar)

Figure 6

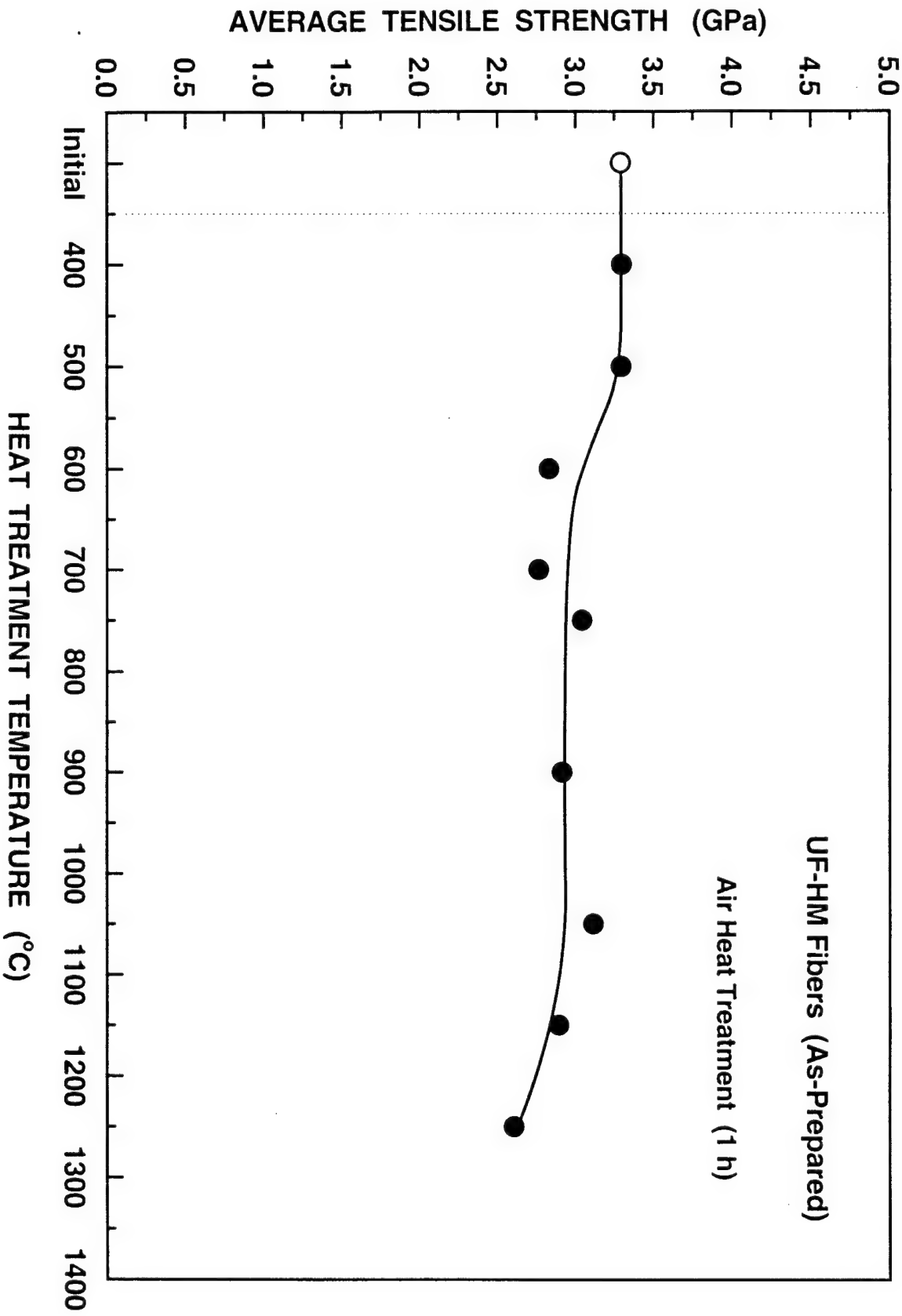
AVERAGE TENSILE STRENGTH (GPa)
0.0
0.5
1.0
1.5
2.0
2.5
3.0
3.5
4.0
4.5
5.0
Initial
400
500
600
700
800
900
1000
1100
1200
1300
1400
HEAT TREATMENT TEMPERATURE (°C)
UF-HM Fibers (As-Prepared)
Air Heat Treatment (1 h)

Figure 7

IN-SITU FIBER COATING

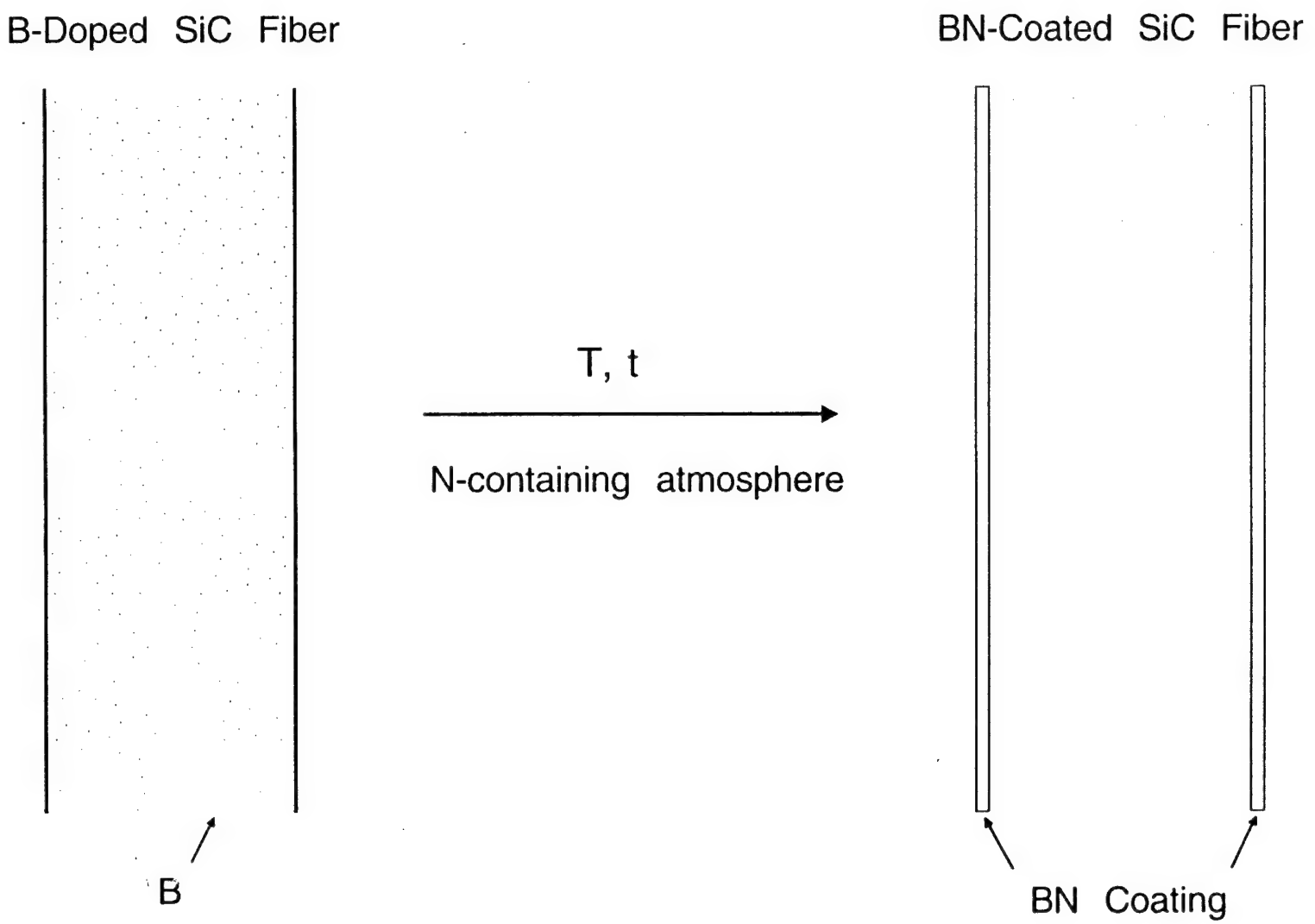

3.2 Modeling and Simulation Studies

Introduction

Modeling and simulation studies are conducted in conjunction with fiber processing and characterization efforts in order to develop an understanding of underlying processes that control high temperature creep and grain growth in SiC fibers. The processes of interest include the following topics:

(1) The development of methodology and potential functions for conducting the simulations for structure and mass transport in SiC
(2) Structure issues:
    (a) SiC grain structure simulation
    (b) Methodology for the formation of grain boundaries and intergranular structures
    (c) Treatment of impurities, vacancies and other structural defects
(3) Mass transport issues:
    (a) The competition between trans-granular lattice diffusion and grain boundary diffusion of each major component of the composition
    (b) The effect of non-stoichiometric distributions of components separated between the effect of excess or vacancies of each component
    (c) The effect of selected dopants used in the experimental studies on both (a) and (b) and calculations of the mass transport properties of the dopants
    (d) Variations of mechanism and activation energies with temperature
(4) Effect of simulated mass transport results on creep behavior
    (a) Development and test of finite element approach
    (b) Application of the range of results obtained in the simulation studies to the finite element model and comparison with experimental results
(5) Examination of the experimental structures and high temperature creep behavior and comparison to the results of modeling studies
    (a) Grain and grain-boundary structure comparisons
    (b) Analysis of experimental results of high temperature creep behavior and development of hypothesis for underlying phenomena
    (c) Comparison with modeling results and test of experimental hypothesis

The approach followed in these studies consists of two parts. In the first approach (Finite Element Approach), it is realized that an atomistic simulation is necessary to model grain and grain-boundary structures and evaluate the change in transport properties in the presence of defects and dopants. However, the experimental work does not directly produce diffusion coefficients. Consequently, we plan to examine changes in transport behavior associated with various structures that reflect measured experimental structures. Simulated transport coefficients will then be used in finite element calculations to extract grain growth and creep coefficients. At this point a comparison is possible with experimental creep data. In the second approach (Comparative Hypothesis Approach), experimental data will be analyzed to develop a theoretical hypothesis of the underlying atomistic processes, then this hypothesis will be tested with the simulation studies. Here only general trends are needed to confirm or modify the experimentally derived hypothesis. However, agreement of simulation results with the hypothesis strengthens understanding of the behavior of the material and can be more valuable in the design of improved processing conditions than numerical comparisons of data. The research conducted is designed to follow both approaches in parallel.

Our modeling studies under this grant have undertaken to examine simulation methodologies in order to determine the most fruitful approach to both grain structure formation and mass transport calculations. It is well recognized that simple molecular dynamics (MD) simulations are inadequate for simulations of either grain boundary structures or mass transport. In the former, the MD method can only access local regions of configurational space centered about a single free energy minimum and cannot jump to other configurational regions about different or equivalent energy minima. In the latter, the simulations are usually too short in time to allow particles to enter a true diffusional regime, and the simulations are mostly dominated by the particle motions around their equilibrium positions.

While many methods have been used to bring together separate grains to form grain boundaries, they usually suffer from the inability of the MD approach to move the grains sufficiently to adjust for any starting bias in the structure. Therefore, the initial structure essentially determines the final structure, as only minor rearrangements are permitted by pure MD methods. This is a result of the limited range of phase space that can be sampled by MD simulations. Monte Carlo (MC) methods are more suitable for finding local and global energy minima. We have examined a recently developed method that combines Monte Carlo selection of structures with MD simulations of global structural changes. This method, Hybrid Monte Carlo (HMC), allows a rapid scan of configurational space, while allowing for particle dynamics to select suitable rearrangements of the structure. This approach has great promise in the development of complex structures such as grain boundaries.

The simulation of diffusion at the atomic level is one of the most difficult problems in materials modeling. It requires accurate accounting of thermal vibrations of large ensembles of particles and it requires following particle motions over long time periods to reach the transport regime. MD simulations can accurately describe thermal particle motions, however, they are inadequate in covering the sufficiently long time periods required to observe true transport, especially if there are several species involved and there is a considerable difference in transport coefficient between the species.

Results To Date

HMC Simulations

Hybrid Monte Carlo simulations [18] are being developed for use in both the simulation of grain boundary structures and in calculations of diffusion coefficients. The details of the work undertaken are given below:
(a) Force function: The development of force functions is a long process. Prior studies by Yip et al [19] have shown that the Tersoff potential [20] with an important modification introduced by Yip and co-workers does an excellent job of representing the mechanical properties of SiC. Consequently, we have chosen to follow that work and use the Tersoff potential for the HMC simulations.
(b) HMC Simulation: In order to develop an adequate algorithm for using HMC simulations, we worked with a perfect SiC crystal heated to temperatures between 1700 and 2700°C. The sample size was initially 64 particles, then increased to 2064 particles. Interatomic forces derived from the Tersoff potential were used and the Verlet algorithm was used in the MD simulations.

The HMC simulation operates by conducting a selected number of MD time steps to allow a

...re to rearrange according to Newton's Laws. After this fixed time, a MC Metropolis ...rison is conducted on the new structure and the state is either accepted or rejected. If the state ...pted, the velocities of the particles are selected from a Maxwell distribution and another set ... steps are taken to allow the structure to evolve again. If the state is rejected, the calculations ... to the previous structure; a new set of velocities is selected from a Maxwell distribution and ...alculations are conducted from that structure. The Metropolis step allows increasing the MD ... step beyond that normally used (15 to 50 times) and it is this ability which allows for longer ...mulations in the same computer time period as normal MD simulations. By scrambling the velocities at each MC interval, the system is thrown into different regions of phase space and samples different configurations. The result is that HMC undergoes global rearrangements, samples a broad region of phase space and covers time more efficiently than MD simulations. The Hybrid Monte-Carlo approach has the ability to maintain ergodicity in a system with harmonic degrees of freedom, while at the same time providing atomic trajectories. In most comparisons, HMC reaches well into the steady-state diffusion regime, in the same computer run time that simple molecular dynamics only achieves random attempts to leave the starting position.

Our current studies are designed to develop grain boundary structures by allowing for major rearrangements of the orientation of adjacent grains. In addition, we have examined particle transport as defined by the HMC approach. Currently, we use a calculation of the rejection rate at the MC interval to determine the length of the time steps. We have found that, at elevated temperatures (near 2,000°C), time steps between 15 and 20 times longer than the MD time step are acceptable, thus run durations 15-20 times longer may be reached in the same amount of computer time. The HMC runs are conducted to determine comparative diffusion coefficients for the Si and C atomic species within a grain, in several grain-boundary structures, and in the presence of boron and nitrogen impurities both in the grain and grain boundary.

Molecular dynamics and Hybrid Monte-Carlo programs for conducting simulations have been developed and comparison runs have been performed on single crystal cubic SiC grains at several temperatures using both methods. The initial tests were reliability runs with the two methods to determine long time and high temperature stability of the potentials used. (We have used both the Tersoff potential [20] and the high temperature modification developed by Yip et al. [19]) The results show reasonable stability over long times. The results show a striking improvement in the calculation of diffusion coefficient by the use of HMC over the MD approach, thus confirming our expectations. We are now conducting simulations of diffusion of Si and C atoms in the β-SiC structure with thermal and a variety of **non-thermal** vacancy defect concentrations (high Si vacancy concentrations), in order to determine their effect on diffusion coefficient and diffusion activation energy.

Sample results of the HMC runs are given in Fig. 8 as energy vs time, showing the expected asymptotic approach to a constant energy and in Fig. 9 as particle displacements at 1700°C. In this approach, since the velocities are scrambled at each MC interval, the passage of time is not realistic. Consequently, the calculated diffusion coefficients are not numerically meaningful, however, others have shown that the relative comparison of the diffusion coefficients from different species have significance. Our studies clearly show an increased diffusion for carbon over silicon and a reasonable activation energy for the change in diffusion for the two species as a function of temperature. These results are preliminary as we plan to use larger ensembles and longer simulation times. However, they show that the approach has promise.

Figure 8

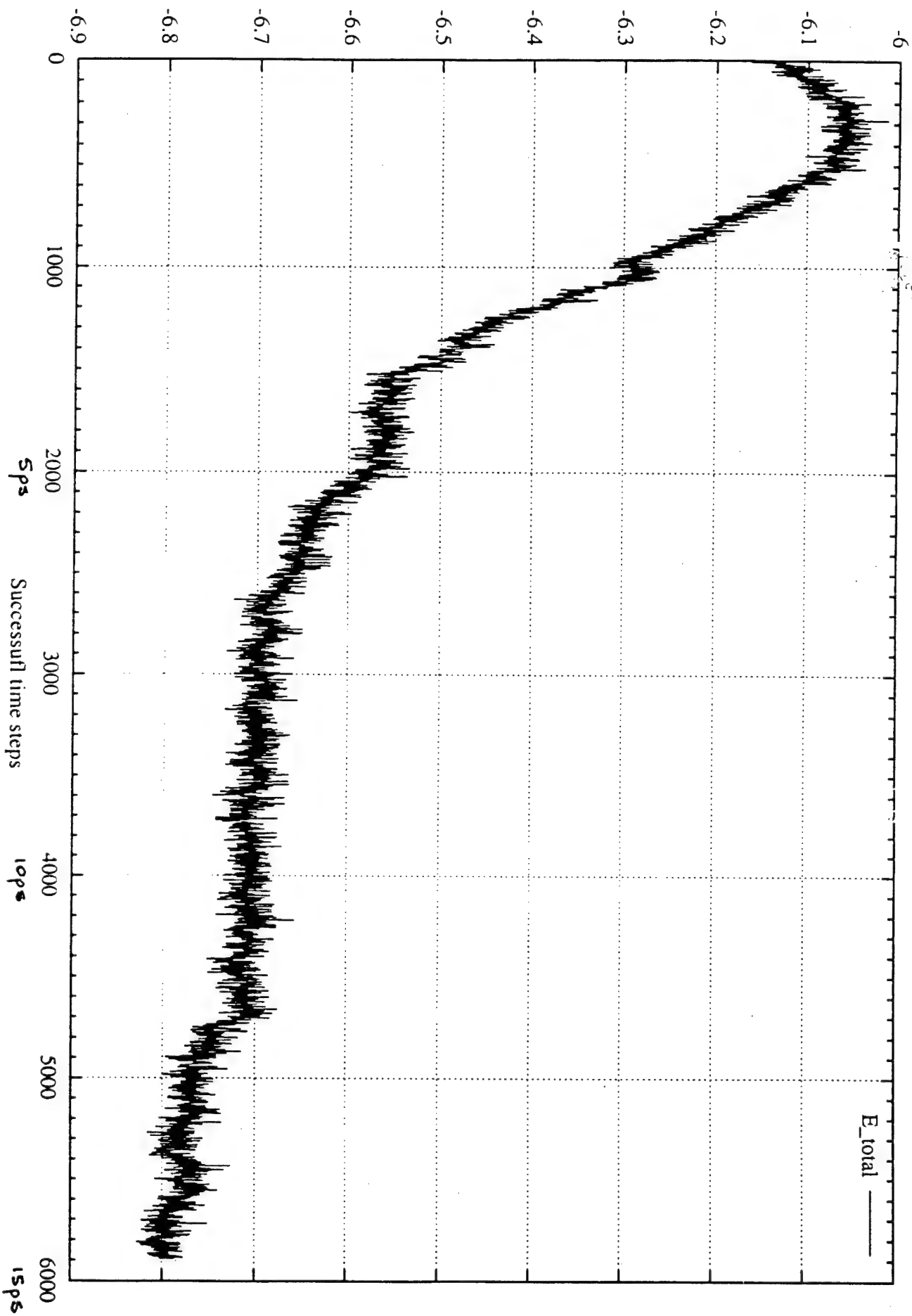
TOTAL ENERGY
E_total
-6
-6.1
-6.2
-6.3
-6.4
-6.5
-6.6
-6.7
-6.8
-6.9
0
1000
2000
3000
4000
5000
6000
Successful time steps
5ps
10ps
15ps

Figure 9

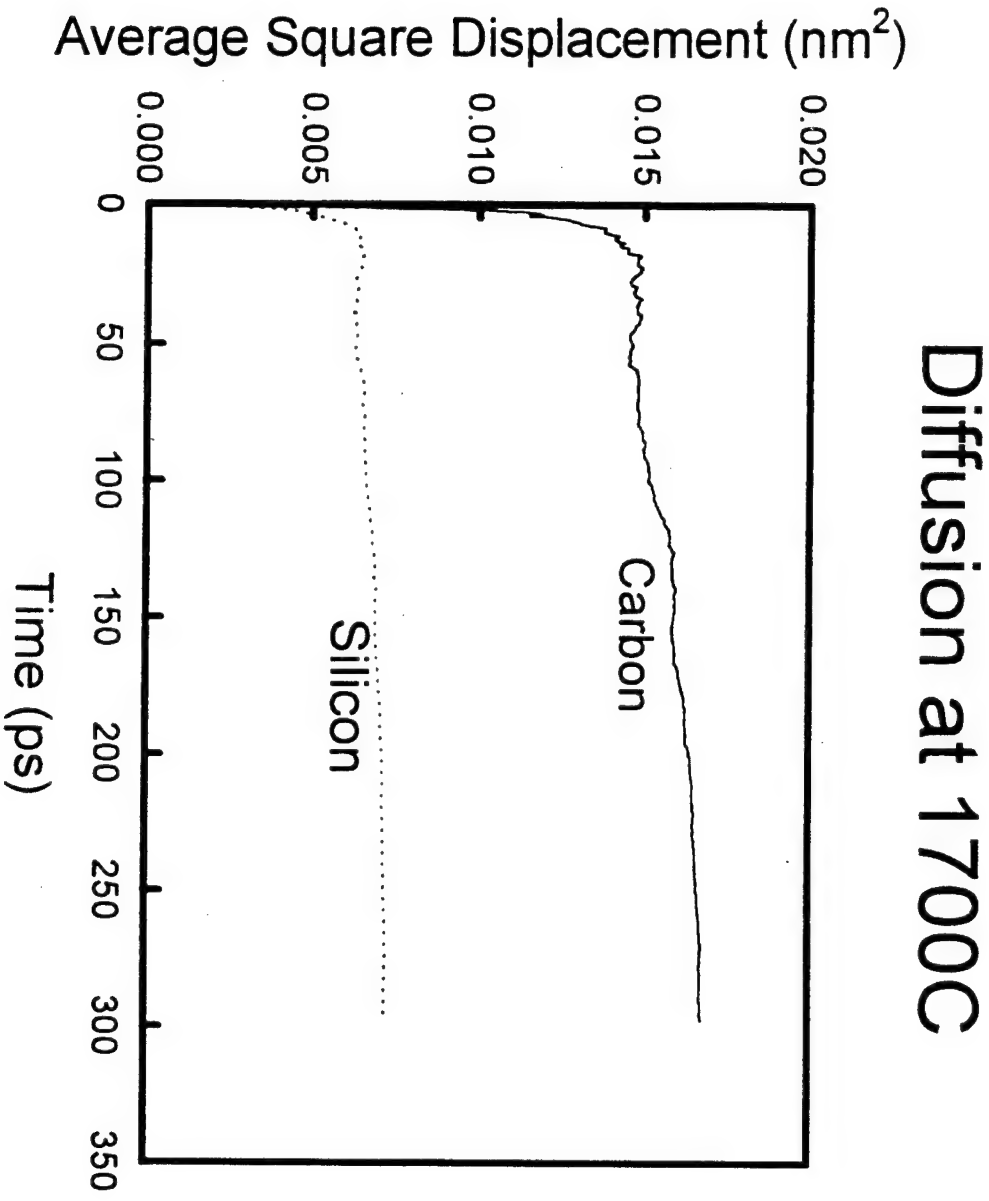
Diffusion at 1700C
Average Square Displacement (nm²)
0.000
0.005
0.010
0.015
0.020
0
50
100
150
200
250
300
350
Time (ps)
Carbon
Silicon

Finite Element Analysis

Finite Element studies are using structures developed to mimic experimental micrographs of SiC fibers obtained from our own research efforts. All grains have been designed to have the same size. Size variations will be introduced later to determine if they have any effect on behavior. The finite element studies offer great flexibility in that wide variations in structures or diffusion coefficients may be input into the calculations and one may then examine the results of the speculation about the effects of these broad variations on the grain growth and creep behavior of the material. From these, we can determine whether the observed experimental effects can be explained by the changes in input conditions, and whether it is possible to achieve materials variations that produce the desirable input conditions.

We have examined finite-element and finite-difference analyses in order to develop a method for calculating creep behavior for a polycrystalline structure in which the grain boundary diffusion is different from the intragranular diffusion. So far, we have examined the Abacus program [21] and found it suitable for the simulations. We have also developed both cubic and hexagonal grids to simulate grain structures. The simulations are currently using intragranular diffusion. We will add grain boundary diffusion processes to evaluate the differences. The simulations follow a method pioneered by Berdichevsky et al. [22] The method balances the applied stress with the flow of vacancies (creep) along the tensile stress direction. We currently use two-dimensional simulations, since these will capture the salient characteristics of the process, then we plan to follow up by looking for differences in 3-D simulations.

For a 2-dimensional stress application, if D is the rate-controlling effective diffusion coefficient, E is Young's modulus, the width of the sample is A and the length is L, the time-dependent strain or creep $\epsilon(t)$ may be written as:

$$\varepsilon(t) = \frac{8\sigma}{\pi^2 AE} \sum_{n} \frac{1}{(2n+1)^2} \left[1 - e^{-\left\{ (2n+1)^2 \left(\frac{\pi^2 ADt}{4L^2} \right) \right\}} \right]$$

Finite-Element (FE) simulations are under way to relate input diffusion coefficients to resultant creep behavior as a function of applied stress and temperature through D. Grain structures assumed so far have been hexagonal. The FE simulations will use atomic diffusion coefficients obtained from the atomistic simulations with structures obtained from the experimental measurements of the SiC fibers to produce time-dependent creep simulations. These simulations are then compared with experimentally determined behavior in order to evaluate the accuracy of the modeling methods and to sort out the mechanisms underlying the creep process in the SiC fibers.

Conducting FE simulations also allows us to change input parameters over a wide range even beyond the values obtained from the simulations in order to determine what structural properties have the most influence on the resultant creep behavior. From these results, we expect to feed back to the experimental programs guidelines for structural changes which will impact improvements in the high-temperature mechanical behavior of SiC fibers. (Throughout the report, we limit our work to SiC fibers because, we expect that since bulk SiC has a very different structure (larger grains), its creep behavior will be drastically different.)

Comparative Hypothesis Approach

This approach consists of conducting experimental runs with controlled variations in the conditions in order to produce data that infer certain processes. From these data, we develop a **hypothesis** about the behavior of the experimental system. The simulation experiments are then used to test the range of reliability of the single hypothesis or the competing possible hypotheses that explain the data. From the results will come first a test and then a refining of the hypothesis, and an inference about which processing controls must be applied or changed in order to improve the characteristics and behavior of the SiC fibers.

For example, recent experimental results obtained in our labs show that fibers with excess carbon have smaller grains and exhibit less creep than stoichiometric fibers. Micrographs show that the excess carbon forms graphitic or amorphous carbon grains in the SiC structure, consequently, one may assume for the **hypothesis** that excess carbon is present in the grain boundaries as well as within the grains. In the latter, the excess carbon causes Si vacancies which are known to enhance Si intragranular diffusion [23, 24]. From the former, one can deduce that the grain boundary diffusion of Si is essentially arrested since it would react with the excess carbon present. Since grain growth and creep are fully controlled by Si diffusion either through the grains or the grain boundary, the result of decreased grain growth and creep therefore is a consequnce of a decrease in Si diffusion at the grain boundary.

Measurements by Davis et al. [23] have shown that the intragranular diffusion coefficients of Si and C vary such that Si is slower than C at temperatures in the range of our measurements 1700-2000°C. Grain boundary diffusion data is less available. These comparisons will be examined in the modeling effort.

Up to now, the modeling studies have ignored the very evident graphitic phase present in the high-carbon fibers. Its effect can be divided into two parts: (1) changes in the atomic diffusion coefficients either in the bulk due to excess Si vacancies or in the grain boundary due to excess carbon, and (2) diffusion and creep effects that involve the graphitic phase itself. The case of excess Si vacancies or excess grain boundary carbon due to high carbon content is being examined in the ongoing work. Simulations of the behavior of at the graphitic phase have not begun due to a lack of tested interatomic potentials. We are examining several candidate potentials at this time, to determine which one is most useful.

4.0 REFERENCES

1. M. Takeda, Y. Imai, H. Ichikawa, and T. Ishikawa, Ceram. Eng. Sci. Proc., 12 [7-8] 1007-1018 (1991).
2. M. Takeda, J. Sakamoto, A. Saeki, Y. Imai, and H. Ichikawa, Ceram. Eng. Sci. Proc., 16 [4] 37-44 1995.
3. M. Takeda, J. Sakamoto, A. Saeki, and H. Ichikawa, Ceram. Eng. Sci. Proc., 17 [4] 35-43 1996.
4. J. Lipowitz, J.A. Rabe, and G.A. Zank, Ceram. Eng. Sci. Proc., 12 [9-10] 1819-1831 (1991).
5. J. Lipowitz, J.A. Rabe, G.A. Zank, A. Zangvil and Y. Xu, Ceram. Eng. Sci. Proc., 18 [3] 147-157 (1997).
6. Wm. Toreki, C.D. Batich, M.D. Sacks, M. Saleem, G.J. Choi, and A.A. Morrone, Composites Sci. Technol., 51 145-159 (1994).
7. M.D. Sacks, A.A. Morrone, G.W. Scheiffele, and M. Saleem, Ceram. Eng. Sci. Proc., 16 [4] 25-35 (1995).
8. G.N. Morscher and J.A. DiCarlo, J. Am. Ceram. Soc., 75 [1] 136-140 (1992).
9. E. Serrano and M.D. Sacks, unpublished work.
10. G. Chollon, R. Pailler, R. Naslain, and P. Olry, pp. 299-302 in *High-Temperature Ceramic-Matrix Composites II: Manufacturing and Materials Development*, Ceram. Trans., Vol. 59. Edited by A.G. Evans and R. Naslain. American Ceramic Society, Westerville, OH, 1995.
11. G.A. Staab and M.D. Sacks, unpublished work
12. R. Bodet, X. Bourrat, J. Lamon, and R. Naslain, J. Mater. Sci., 30 661-677 (1995).
13. H.M. Yun, J.C. Goldsby, and J.A. DiCarlo, pp. 331-336 in *High-Temperature Ceramic-Matrix Composites II: Manufacturing and Materials Development*, Ceram. Trans., Vol. 59. Edited by A.G. Evans and R. Naslain. American Ceramic Society, Westerville, OH, 1995.
14. J.A. DiCarlo, Composites Sci. Technol., 51 213-222 (1994).
15. G.N. Morscher and J.A. DiCarlo, Proceedings of the NASA 6th Annual HITEMP Review, Cleveland, OH, 1993.
16. G.N. Morscher, unpublished results.
17. F. Frechette, B. Dover, V. Venkateswaran, and J. Kim, Ceram. Eng. Sci. Proc., 12 [7-8] 992-1006 (1991).
18. S. Duane, A. D. Kennedy, B. J. Pendleton and D. Roweth, Phys.Lett. B, 195 216 (1987); D. W. Heerman, P. Nielaba and M. Rovere, Comput. Physics Comm., 60 311 (1990).
19. M. Tang and S. Yip, Phys. Rev. B, 52 15150 (1995).
20. J. Tersoff, Phys. Rev. Lett., 61 2879 (1988).
21. Hibbit, Karlsson, and Sorensen, Abaqus, Pawtucket, RI, 1997.
22. V. Berdichevsky, P. Hazzeldine and B. Shoykhet, Int. J. Engng. Sci., 35 1003 (1997).
23. J. D. Hong and R. F. Davis, J. Am. Ceram. Soc., 63 546 (1980); J. Mater. Sci., 16 2485 (1981).
24. D. P. Birnie, J. Am. Ceram. Soc., 69 C-33 (1986).

5.0 APPENDIX

pended Publications

"Polymer-Derived SiC-Based Fibers with High Tensile Strength and Improved Creep Resistance," to be published in Ceram. Eng. Sci. Proc., Vol. 19, 1998.

"Effect of Composition and Heat Treatment Conditions on the Tensile Strength and Creep Resistance of SiC-Based Fibers," to be published in J. Eur. Ceram. Soc., 1999.

Presented at the 22nd Annual Cocoa Beach Conference and Exposition on Composites, Advanced Ceramics, Materials and Structures, Cocoa Beach, FL, January 20-24, 1998 (Paper No. C-132-98). To be published in Ceram. Eng. Sci. Proc., Vol. 19, 1998.

POLYMER-DERIVED SiC-BASED FIBERS WITH HIGH TENSILE STRENGTH AND IMPROVED CREEP RESISTANCE

Michael D. Sacks, Gary W. Scheiffele, Lan Zhang, and Yunpeng Yang
University of Florida, Gainesville, FL 32611

John J. Brennan
United Technologies Research Center, East Hartford, CT 06108

ABSTRACT

Fine-diameter (~10-15 μm), polymer-derived, SiC-based fibers with carbon-rich and near-stoichiometric compositions were prepared and characterized. Tensile strengths and creep resistance were evaluated for as-fabricated fibers and for fibers given heat treatments at temperatures up to 1950°C. The creep resistance was assessed using the bend stress relaxation (BSR) method developed by Morscher and DiCarlo. Fibers showed excellent strength retention after heat treatments in argon (for 1 h) at temperatures up to 1700°C for the carbon-rich ("UF") fibers and up to 1800°C for the near-stoichiometric ("UF-HM") fibers. Creep resistance of the as-fabricated fibers was greatly improved by high temperature annealing treatments. Heat-treated UF fibers could be prepared with ~3 GPa tensile strengths and BSR creep behavior which was similar to that reported for Hi-Nicalon™ Type S fibers. Heat-treated UF-HM fibers were also prepared with ~3 GPa tensile strengths, while BSR results showed that the creep resistance was significantly better than that reported for Hi-Nicalon™ Type S fibers. It was also shown that the UF-HM fibers could be coated with hexagonal BN using an in-situ processing method.

INTRODUCTION

There has been considerable interest in recent years in producing SiC-based fibers with improved thermomechanical properties. Much of the effort in this area has been directed toward fabrication of fine-diameter, high-strength, polymer-derived fibers which have low oxygen content.[1-14] The development of such fibers with both carbon-rich and near-stoichiometric compositions have been reported by several research groups, including those at Nippon Carbon Co. (Hi-Nicalon™ and Hi-Nicalon™ Type S fibers)[1-6], Dow Corning Co. (Sylramic™ fibers)[7-10], and the University of Florida (UF and

UF-HM fibers).[11-14] All of these fibers show significantly improved thermomechanical properties compared to fibers which contain large amounts of oxygen, such as Nicalon™ and Tyranno™ fibers.

In this study, the tensile strength and creep resistance of carbon-rich UF fibers and near-stoichiometric UF-HM fibers were evaluated before and after heat treatments at temperatures up to 1950°C. The creep resistance was assessed using the bend stress relaxation (BSR) method of Morscher and DiCarlo.[15]

This study also reports the development of boron nitride (BN) coatings on the UF-HM SiC fibers. Well-crystallized hexagonal BN layers were formed by an in-situ processing method.

EXPERIMENTAL

The development of polymer-derived UF and UF-HM fibers has been reported previously.[11-14] Fibers were fabricated using a high-molecular-weight polycarbosilane (PCS) polymer as the primary ceramic precursor. (The infusible PCS polymers were prepared by pressure pyrolysis of polydimethylsilane.) Fine-diameter fibers were formed by dry spinning of concentrated PCS-based polymer solutions. The polymeric fibers were decomposed to SiC-based ceramics by pyrolysis in an inert atmosphere. Carbon-rich fibers (designated "UF fibers") were initially processed at temperatures in range of 1000-1200°C, while the near-stoichiometric fibers (designated "UF-HM fibers") were fabricated at higher temperatures ($\geq$1750°C). Boron additions were used in the latter fibers, both as a sintering aid and as the boron source for the formation of BN coatings by in-situ processing.

Conventional and high resolution transmission electron microscopy (TEM and HRTEM) were used to characterize the fiber microstructure. The phases present were determined by X-ray diffraction (XRD) and electron diffraction. Elemental analyses for Si,C,O, and N were carried out using electron microprobe analysis (EMA). Oxygen concentrations were also determined by neutron activation analysis, NAA, (Nicolet Electron Services, San Diego, CA). NAA was also used to determine boron concentrations (University of Missouri Research Reactor, Columbia, MO). Fiber apparent densities were determined by a sink-float method (ASTM procedure D3800-79).[16]

Single-filament tensile strengths were determined at room temperature according to ASTM procedure D3379.[17] The fiber gage length was 25 mm. The creep behavior of fibers was assessed using the bend stress relaxation (BSR) method.[15] In this method, stress relaxation values (designated as "M" values) are determined based on the extent of permanent deformation that occurs when fibers are heat treated under an applied bending load. An M value which approaches 1 indicates that no permanent (creep) deformation occurred during the high temperature annealing, while an M value of 0 indicates that the stress completely relaxed. Hence, fibers are considered more thermally stable against creep as the M values increase from 0 to 1.

RESULTS AND DISCUSSION

High-Strength, Creep-Resistant UF Fibers and UF-HM Fibers

Table 1 summarizes the characteristics of typical as-fabricated UF fibers (carbon-rich) and UF-HM (near-stoichiometric) fibers.

The as-pyrolyzed UF fibers had normalized Si/C weight ratios in the range of ~59-62 wt% Si/38-41 wt% C, with an average ratio (determined from 8 samples) of ~60.5 wt% Si/~39.5 wt% C. Hence, these fibers are highly carbon-rich relative to stoichiometric SiC (~70 wt% Si/~30 wt% C). Oxygen was present in the fiber as an impurity picked up during various stages of processing.[12] The concentrations usually did not exceed 1.5 wt% and were more typically in the range of ~0.5-1.0 wt%. Some of the fibers were doped with small amounts of boron. The phases present in the UF fibers were β-SiC and XRD-amorphous carbon. TEM and XRD line-broadening measurements indicated that the β-SiC crystallite sizes were less than 5 nm. Fiber apparent densities were in the range of ~2.5-2.7 g/cm^3. The relatively low densities are consistent with the large amount of carbon present in the fibers and the weakly crystalline nature of the SiC grains. (Well-crystallized, high purity SiC has a density of ~3.21 g/cm^3.)

Figure 1A shows a histogram plot of the average room temperature tensile strengths obtained for 43 separate sets of UF fibers. (In most cases, $\geq$15 fibers were tested for each set.) The mean tensile strength was 3.23 GPa (468 ksi). The mean diameter for these test sets was 12.6 μm. Previous fractography studies on similar fibers indicated that the strength-controlling flaw sizes were mostly in the range of ~0.2-0.3 μm.[18] This corresponds closely to the smallest pore sizes of the filters (nominal sizes were 0.1-0.2 μm) that were used to prepare the spinning solutions for fiber fabrication. Hence, it is possible that the tensile strength of the UF fibers is controlled primarily by processing-related particulates (i.e., impurity particles, polymer "microgel" particles, etc.).

The near-stoichiometric UF-HM fibers had normalized Si/C weight ratios mostly in the range of ~67-70 wt% Si/30-33 wt% C, with an average composition (determined from >25 samples) of ~68.5 wt% Si/~31.5 wt% C. This indicates that the fibers usually contained a small amount of excess carbon. X-ray and electron diffraction analyses of the UF-HM fibers showed that β-SiC was the primary phase in the fibers, although traces of the alpha phase were observed in some fibers. The SiC grain sizes were generally in the range of ~0.05 - 0.3 μm, although grains as large as ~0.5-1.0 μm were occasionally observed. Residual carbon was not detected by a standard XRD powder diffraction method, but was observed by TEM. HRTEM analysis showed the stacked hexagonal structural units with interplanar spacing of 0.34 nm that are associated with graphitic carbon. EMA analysis for oxygen and nitrogen showed that concentrations were less than the resolution limit for the technique (typically $\leq$0.2 wt%). The boron concentrations were usually on the order of 1 wt%, although fibers with range of boron concentrations (i.e., ~0.1 - 3.0 wt%) were also prepared.

The apparent densities of the UF-HM fibers were usually in the range of 3.1-3.2

TABLE 1. TYPICAL FIBER CHARACTERISTICS

UF Fibers (Carbon-Rich Composition)		
Elemental Analysis:	Si/C ratio:	~59-62 wt% Si/~38-41 wt% C
	Oxygen:	~0.5 - 1.5 wt%
	Boron:	~0-1 wt%
Phases:	weakly-crystalline β-SiC, XRD-amorphous Carbon	
SiC Grain Size:	$\leq$5 nm	
Apparent Density:	~2.5-2.7 g/cm^3	
Diameter:	~10-15 μm	
Tensile Strength:	~400-500 ksi (~2.8-3.5 GPa)	
UF-HM Fibers (Near-Stoichiometric Composition)		
Elemental Analysis:	Si/C ratio:	~67-70 wt% Si/~30-33 wt% C
	Boron:	~0.1 - 3.0 wt%
	Oxygen:	$\leq$0.2 wt%
	Nitrogen:	$\leq$0.2 wt%
Phases:	well-crystallized β-SiC trace amounts of graphitic Carbon, α-SiC	
SiC Grain Size:	mostly ~0.05-0.3 μm	
Apparent Density:	~3.1-3.2 g/cm^3	
Diameter:	~10-15 μm	
Tensile Strength:	~300-500 ksi (~2.1-3.5 GPa)	

g/cm^3, with an average value of ~3.15 g/cm^3. The latter value is 98% of the theoretical value of 3.21 g/cm^3 for fully dense (pore-free), stoichiometric SiC. The density is lower than the theoretical value, at least in part, because of the small amount of residual carbon. In addition, small amounts of fine pores (usually less than 0.1 μm) were occasionally observed (by TEM) at grain junctions.

Figure 1B shows a histogram plot of the average room temperature tensile strengths obtained for 150 separate sets of as-sintered UF-HM fibers. (In most cases, $\geq$15 fibers were tested for each set.) The mean tensile strength was 2.85 GPa (413 ksi). The mean

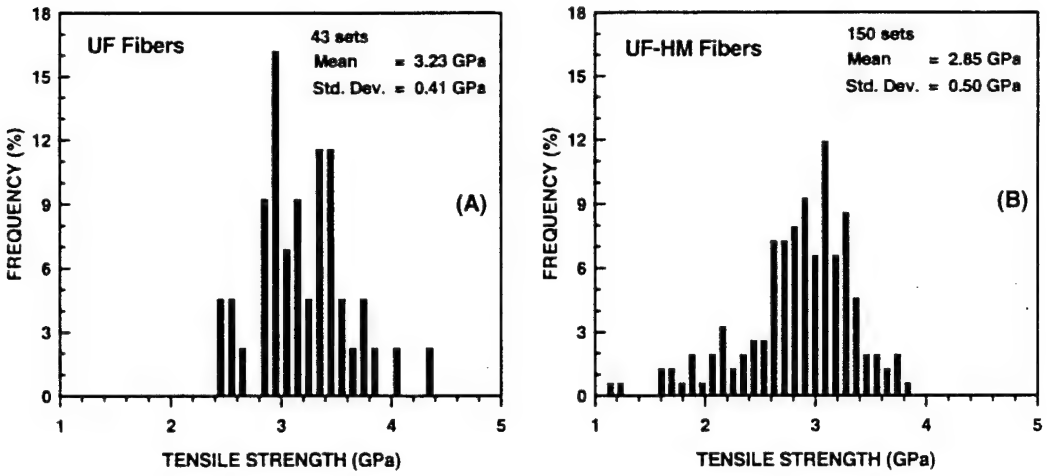

Fig. 1. Histogram plots of frequency vs. tensile strength for (A) UF fibers and (B) UF-HM fibers.

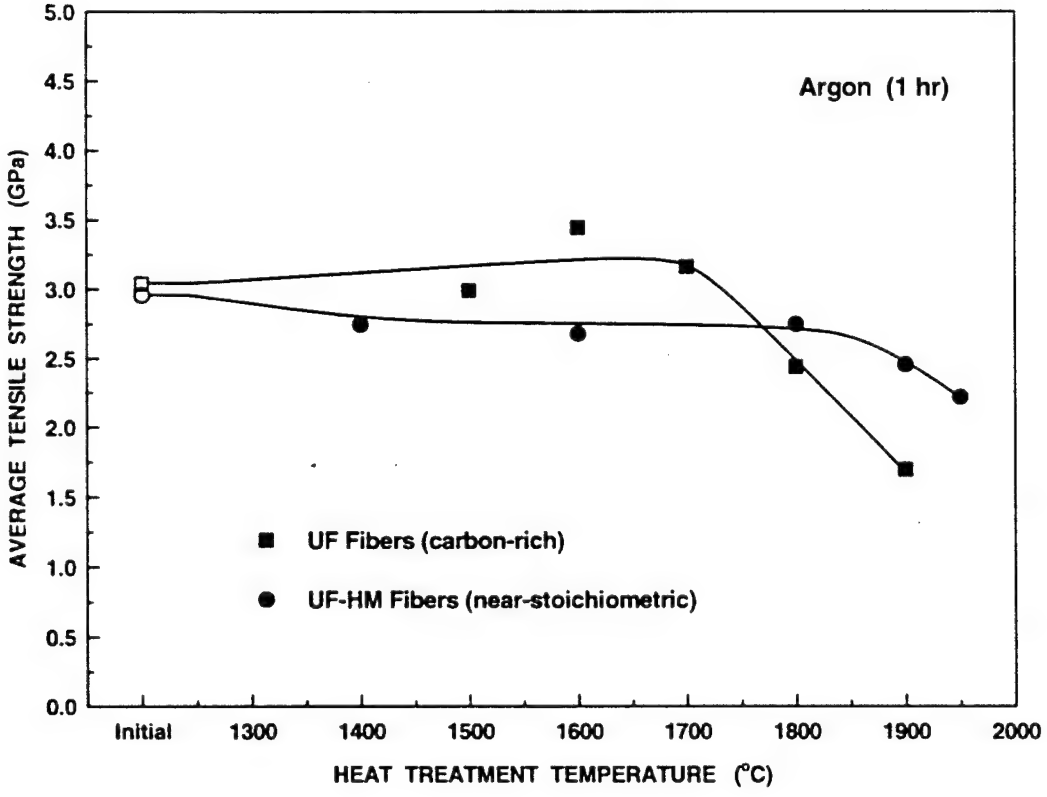

Fig. 2. Plots of average tensile strength vs. heat treatment temperature for UF fibers and UF-HM fibers.

diameter for these test sets was 12.1 μm. The tensile strengths of the UF-HM fibers are probably controlled primarily by larger grains at the fiber surface. (Fracture was generally initiated at the surface, but it was difficult to identify the specific flaws responsible for failure.)

Figure 2 shows room temperature tensile strengths for UF and UF-HM fibers after heat treatments in argon for 1 h at temperatures in the range of 1400-1950°C. The UF-HM fibers retained most of their original strength through heat treatments up to 1800°C and then the strength gradually decreased with heat treatments at higher temperatures (up to 1950°C). The UF fibers showed no loss in strength with heat treatments up to 1700°C and then showed sharper decreases in strength (compared to the UF-HM fibers) with further heat treatments up to 1900°C. Despite these differences, both the UF fibers and the UF-HM fibers show greater retention of their original strengths after high temperature (e.g., $\geq$1600°C) heat treatments in argon compared to the strength retention reported for carbon-rich Hi-Nicalon™ fibers and near-stoichiometric Hi-Nicalon™ Type S fibers, respectively.[4,5,19]

As noted earlier, it is believed that the strength-controlling flaws for the as-prepared UF-HM fibers are larger grains at the fiber surfaces. Therefore, the gradual decrease in tensile strength in the UF-HM fibers after heat treatment in argon at higher temperatures is attributed to grain growth. A small increase in the grain sizes was confirmed by TEM observations on a 1950°C heat-treated sample.[20]

It is not clear why the UF fibers decrease in tensile strength at lower heat treatment temperature (and decrease more sharply with increasing temperature) compared to the UF-HM fibers. For Hi-Nicalon™ fibers, it has been suggested that the strength decreases upon heat treatment in inert atmospheres because of a combination of coarsening of SiC grains and flaw formation resulting from thermochemical degradation reactions.[19] (The presence of small amounts of residual oxygen in the Hi-Nicalon™ fibers is expected to result in the same type of carbothermal reduction reductions that occur in conventional Nicalon™ fibers.[21-24] Such reactions result in weight losses, formation of porosity, and coarsening of SiC grains.[21-24] However, in the case of Hi-Nicalon™ fibers, these effects are much less extensive due to the much lower oxygen content.) Although these strength-degradation mechanisms are not implausible, they do not appear to the likely cause of the strength decay that is observed in Fig. 2 for the UF fibers. This is suggested for the following reasons:

(1) UF fibers undergo SiC grain coarsening during heat treatment which is similar to that observed in Hi-Nicalon[24]; however, the grains remain smaller than the grains observed in the UF-HM fibers. Figures 3A and 3B show TEM micrographs for a UF fiber heat treated for 1 h at 1900°C (in argon) and a UF-HM fiber heat treated for 0.2 h at 1840°C (in argon), respectively. Despite heat treatment at the higher temperature and longer time, the UF fibers have a considerably smaller average grain size compared to the UF-HM fibers. (The relatively slow grain growth in the UF fibers can be attributed to the much larger amount of excess carbon. This is expected to inhibit the Si diffusional transport that is required for SiC grain coarsening.)

(2) The carbothermal degradation reactions arising from the small amounts of residual

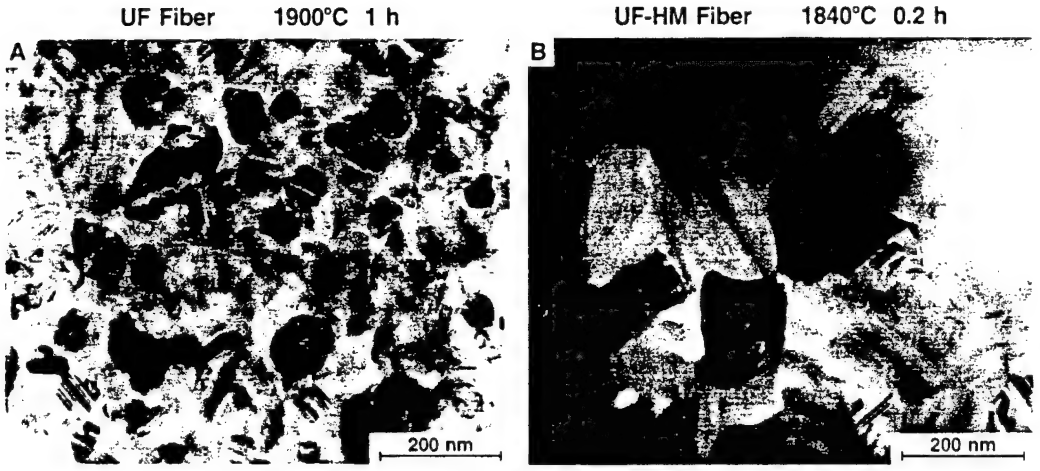

Fig. 3. TEM micrographs for (A) a UF fiber heat treated for 1 h at 1900°C and (B) a UF-HM fiber heat treated for 0.2 h at 1840°C.

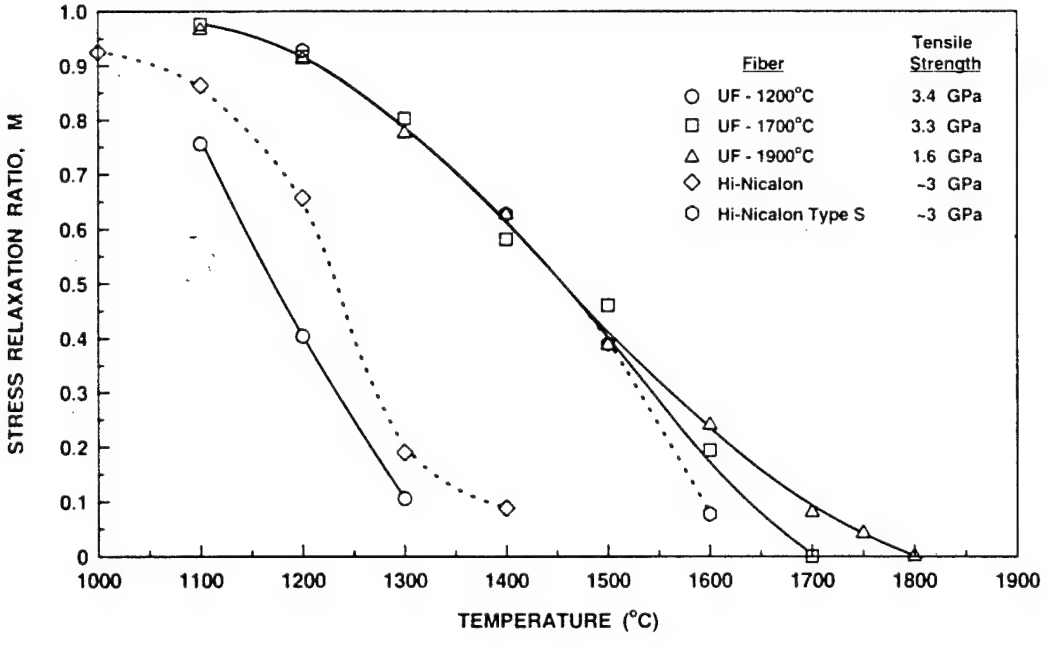

Fig. 4. Plots of stress relaxation ratio, M, vs. heat treatment temperature for as-prepared UF fibers (1200°C), heat-treated UF fibers (1700 and 1900°C), Hi-Nicalon fibers, and Hi-Nicalon Type S fibers.

oxygen are expected to begin at temperatures below 1700°C.[21-24] If these reactions caused significant flaw formation in the UF fibers, then the strength decreases would be expected to begin at lower heat treatment temperatures. Furthermore, scanning electron microscope (SEM) observations of the fibers (including the fracture surfaces) did not reveal the development of any obvious flaws which could account for the sharp decreases in strength with heat treatments above 1700°C.

A possible explanation for the more rapid decay in strength of the UF fibers with heat treatment is the presence of residual tensile stresses at the fiber surface. Such stress might arise due to the mismatch in thermal expansion coefficients between SiC and C. These stresses could become more severe as the SiC/C structure coarsens during heat treatment at higher temperatures. (In addition to growth of the β-SiC grains, the carbon regions grow into larger and more highly ordered domains when PCS-derived carbon-rich SiC fibers are heat treated at temperatures above the original fabrication temperature.[19,25] The growth of the graphitic carbon regions also has significance because graphite has a very large difference in the thermal expansion coefficients for the directions parallel and normal to the hexagonal basal planes.)

The excellent strength retention of the UF and UF-HM fibers after high temperature heat treatments (e.g., compared to fibers such as Hi-Nicalon™ and Hi-Nicalon™ Type S) offers the possibility for improved high-temperature strength retention in ceramic-matrix composites (CMC's) that are fabricated with such fibers. Furthermore, two other advantages can be realized. First, higher temperatures can be used during the processing of CMC's (e.g., to produce matrices with higher relative density) without degradation of the properties of the fibers. Second, it is possible to prepare fibers with improved creep resistance, while still retaining high tensile strength. In regard to the latter consideration, it has been shown that Hi-Nicalon™ and Hi-Nicalon™ Type S fibers become more creep-resistant after annealing heat treatments above the original processing temperature.[6,26] (This may be attributed to the increased grain sizes and/or the more highly crystallized graphitic carbon. Both microstructural changes are expected to inhibit diffusion-controlled creep processes.) The same effect (i.e., improved creep resistance in annealed fibers) was observed in the present study for the UF and UF-HM fibers. Figure 4 shows plots of the bend stress relaxation ratios, M, as a function of the heat treatment temperature for as-pyrolyzed (1200°C) UF fibers and for UF fibers which were given heat treatments for 1 h (in argon) at 1700°C and 1900°C. As expected, substantial increases in M values were obtained for the heat-treated UF fibers. The 1700°C heat-treated UF fibers not only shows greatly improved creep resistance (based on the BSR test results), but also retains high tensile strength.

Figure 4 also includes BSR data reported [6,27-29] for Hi-Nicalon™ and Hi-Nicalon™ Type S fibers. The Hi-Nicalon™ fibers have higher M values (for a given BSR test temperature) compared to the as-prepared UF fibers. This is attributed to a slightly higher initial processing temperature for the Hi-Nicalon™ fibers which, in turn, results in slightly coarser microstructures (including larger SiC crystallite sizes). The 1700°C heat-treated UF fibers have M values comparable or better (for a given BSR test temperature) than the Hi-Nicalon™ Type S fibers. This occurs despite the fact that the

grain sizes are larger for the latter fibers.[6] This observation again suggests that diffusion is inhibited in SiC-based fibers with larger amounts of excess carbon. (This manifests itself not only in the slower coarsening of SiC grains, but also in the improved creep resistance of the fibers.)

Figure 5 shows that the creep resistance (as assessed by the BSR method) for the near-stoichiometric UF-HM fibers can also be improved by annealing heat treatments. In fact, the annealed UF-HM fibers show comparable BSR behavior to that reported [27-29] for much weaker, coarse-grained Carborundum fibers. (The latter fibers were prepared by sintering of SiC powders.[30] This resulted in fibers with considerably larger grain sizes, larger diameters, and rougher surfaces compared to typical polymer-derived SiC fibers. The coarser grain sizes result in fibers with excellent creep resistance, but relatively low tensile strength.)

Takeda et al.[6] have reported that annealing heat treatments can be used to improve the creep resistance of the Hi-Nicalon™ Type S fibers (as assessed by the BSR test). However, these fibers do not retain tensile strengths as high as the UF-HM fibers after the annealing heat treatments. This is illustrated in Fig. 6 which shows plots of tensile strengths vs. M values for Hi-Nicalon™ Type S and UF-HM fibers which were subjected to various annealing heat treatments prior to BSR tests at 1400°C (for 1 h argon). It was possible to produce UF-HM fibers which had 1400°C BSR M values of ~0.9, while still retaining tensile strengths of ~3 GPa. In contrast, 1400°C BSR M values of only ~0.6 were possible in Hi-Nicalon™ Type S fibers which retained tensile strengths of ~3 GPa.

BN-Coated UF-HM fibers

UF-HM fibers with BN surface coatings were prepared by an in-situ process which is schematically illustrated in Fig. 7 (top). Boron-doped fibers were heat treated in a nitrogen-containing atmosphere. BN forms by reaction of boron at the surface with nitrogen in the atmosphere. After the initial reaction at the original SiC fiber surface, it is presumed that the increases in thickness of the coating occur by diffusion of boron from the interior of the fiber to the reaction layer, followed by chemical interdiffusion of boron and nitrogen through the growing BN layer.

Figure 7 (bottom left) shows a TEM micrograph of the BN coatings formed on the UF-HM fibers. Typical coating thicknesses were ~0.1-0.2 μm, although it may be possible to increase the thickness by using SiC fibers with higher initial boron content. Figure 7 (bottom right) shows an HRTEM micrograph of the BN layer. Electron diffraction analysis and lattice spacing measurements showed that the coating layer is hexagonal BN. The HRTEM micrograph also shows that the coating grows such that the hexagonal BN basal planes are oriented mostly perpendicular to the long axis of the UF-HM fibers.

UF-HM fibers prepared with the BN coatings retained high strength (~3 GPa) and excellent creep resistance. The effectiveness of the BN coatings for developing weak fiber/matrix interfaces in CMC's has not yet been evaluated.

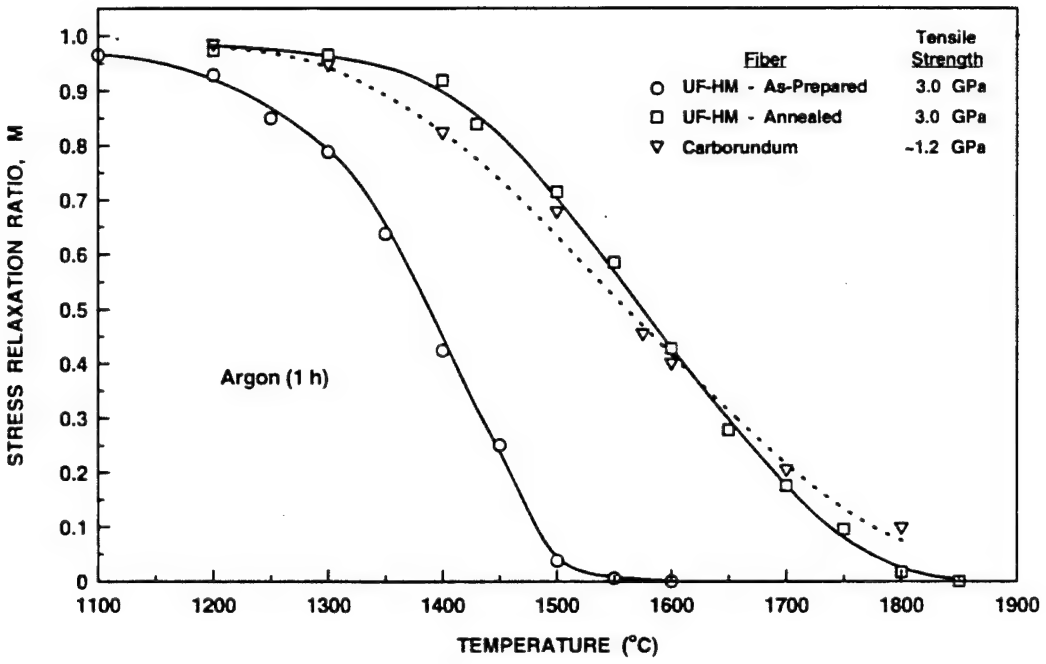

Fig. 5. Plots of stress relaxation ratio, M, vs. heat treatment temperature for as-prepared UF-HM fibers, heat-treated UF-HM fibers, and Carborundum fibers.

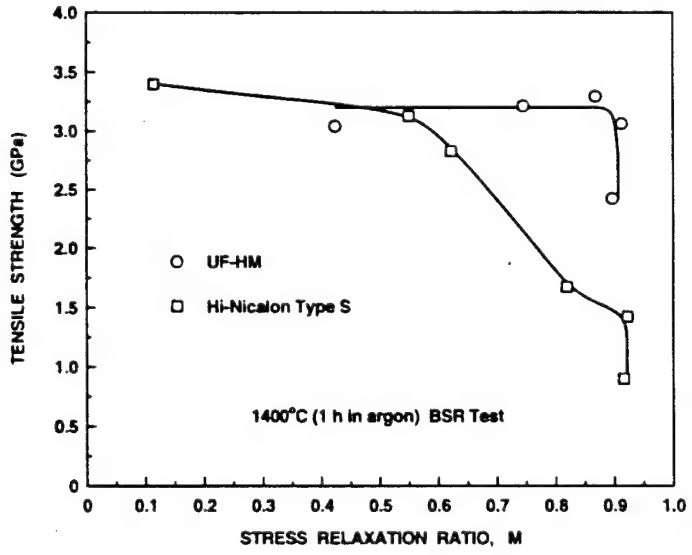

Fig. 6. Plots of tensile strength vs. stress relaxation ratio, M, for UF-HM fibers and Hi-Nicalon Type S fibers which were given varying annealing treatments in order to alter the M values. The BSR test temperature was 1400°C.

IN-SITU PROCESSING OF BN COATINGS

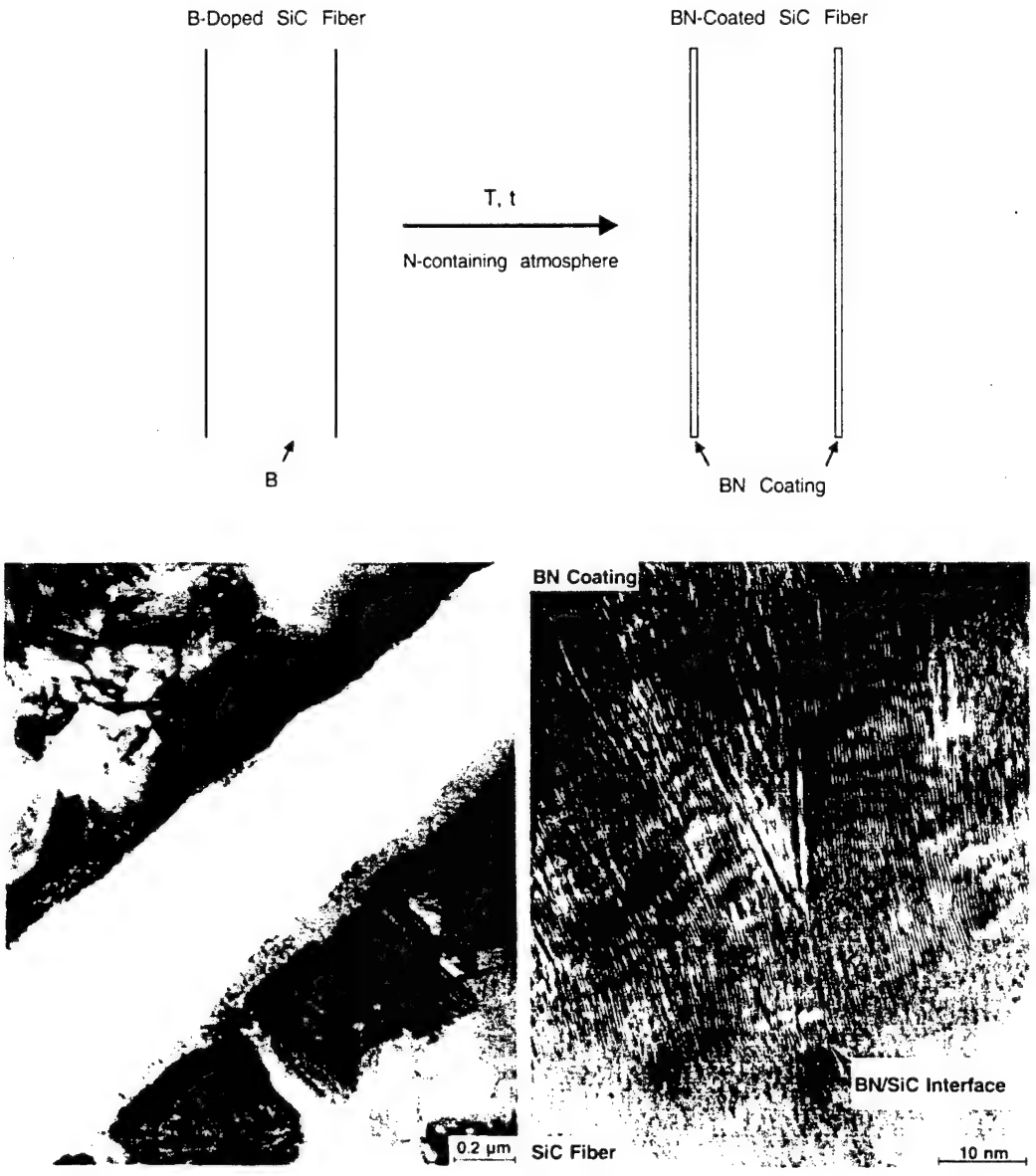

Fig. 7. Top: Schematic illustration of the formation of a BN coating on a SiC fiber by in-situ processing. Bottom left: TEM micrograph showing BN coatings and SiC fiber grains. Bottom right: HRTEM micrograph showing the BN coating/SiC fiber interface and the lattice planes of the BN coating. The BN basal planes grow with an orientation that is mostly perpendicular to the long axis of the SiC fiber.

ACKNOWLEDGEMENTS

The authors thank J.A. DiCarlo and G.N. Morscher of the NASA Lewis Research Center for assistance with the BSR measurements and helpful discussions; G.A. Staab, M. Saleem, G. Brubaker, T.J. Williams, and A.A. Morrone of the University of Florida for experimental contributions; and D. Kutikkad of the University of Missouri for the boron analysis by NAA. Support for this work by the Advanced Research Projects Agency and the Office of Naval Research (N00014-91-J-4075, N00014-93-1-0853), Air Force Office of Scientific Research, (F49620-94-1-0429, F49620-97-1-0095), and the IHPTET Fiber Development Consortium (IHP-UFLA-93A374-005, IHP-MMM-96A374-011) is gratefully acknowledged.

REFERENCES

1. M. Takeda, Y. Imai, H. Ichikawa, and T. Ishikawa, "Properties of the Low Oxygen Content SiC Fiber on High Temperature Heat Treatment", Ceram. Eng. Sci. Proc., 12 [7-8] 1007-1018 (1991).
2. M. Takeda, Y. Imai, H. Ichikawa, T. Ishikawa, N. Kasai, T. Suguchi, and K. Okamura "Thermal Stability of the Low Oxygen Content Silicon Carbide Fibers Derived from Polycarbosilane," Ceram. Eng. Sci. Proc., 13 [7-8] 209-217 (1992).
3. T. Ishikawa, "Recent Developments of the SiC Fiber Nicalon and Its Composites, Including Properties of the SiC Fiber Hi-Nicalon for Ultra-High Temperature," Composites Sci. Technol., 51 135-144 (1994).
4. M. Takeda, J. Sakamoto, Y. Imai, H. Ichikawa, and T. Ishikawa, "Properties of Stoichiometric Silicon Carbide Fiber Derived from Polycarbosilane," Ceram. Eng. Sci. Proc., 15 [4] 133-141 1994.
5. M. Takeda, J. Sakamoto, A. Saeki, Y. Imai, and H. Ichikawa, Ceram. Eng. Sci. Proc., "High Performance Silicon Carbide Fiber Hi-Nicalon for Ceramic Matrix Composites," 16 [4] 37-44 1995.
6. M. Takeda, J. Sakamoto, A. Saeki, and H. Ichikawa, Ceram. Eng. Sci. Proc., "Mechanical and Structural Analysis of Silicon Carbide Fiber Hi-Nicalon Type S," 17 [4] 35-43 1996.
7. J. Lipowitz, J.A. Rabe, and G.A. Zank, "Polycrystalline SiC Fibers from Organosilicon Polymers," Ceram. Eng. Sci. Proc., 12 [9-10] 1819-1831 (1991).
8. Y. Xu, A. Zangvil, J. Lipowitz, J.A. Rabe, and G.A. Zank, "Microstructure and Microchemistry of Polymer-Derived Crystalline SiC Fibers," J. Am. Ceram. Soc., 76 [12] 3034-3040 (1993).
9. J. Lipowitz, T. Barnard, D. Bujalski, J.A. Rabe, G.A. Zank, Y. Xu, and A. Zangvil, "Fine-Diameter Polycrystalline SiC Fibers," Composites Sci. Technol., 51 167-171 (1994).
10. J. Lipowitz, J.A. Rabe, G.A. Zank, A. Zangvil and Y. Xu, "Structure and Properties of Sylramic™ Silicon Carbide Fiber – a Polycrystalline, Stoichiometric β-SiC Composition," Ceram. Eng. Sci. Proc., 18 [3] 147-157 (1997).
11. Wm. Toreki, G.J. Choi, C.D. Batich, M.D. Sacks, and M. Saleem, "Polymer-Derived Silicon Carbide Fibers with Low Oxygen Content," Ceram. Eng. Sci. Proc., 13 [7-8] 198-208 (1992).
12. Wm. Toreki, C.D. Batich, M.D. Sacks, M. Saleem, G.J. Choi, and A.A. Morrone, "Polymer-Derived Silicon Carbide Fibers with Low Oxygen Content and Improved Thermomechanical Stability," Composites Sci. Technol., 51 145-159 (1994).
13. M.D. Sacks, A.A. Morrone, G.W. Scheiffele, and M. Saleem, "Characterization of

Polymer-Derived Silicon Carbide Fibers with Low Oxygen Content, Near-Stoichiometric Composition, and Improved Thermomechanical Stability," Ceram. Eng. Sci. Proc., 16 [4] 25-35 (1995).

14. M.D. Sacks, G.W. Scheiffele, M. Saleem, G. Staab, T.J. Williams, and A.A. Morrone, "Polymer-Derived Silicon Carbide Fibers with Near-Stoichiometric Composition and Low Oxygen Content," pp. 3-10 in *Ceramic Matrix Composites - Advanced High Temperature Structural Materials*, Mat. Res. Soc. Symp. Proc., Vol. 365. Edited by R.A. Lowden, M.K. Ferber, J.R. Hellmann, S.G. DiPietro, and K.K. Chawla. Materials Research Society, Pittsburgh, PA, 1995.
15. G.N. Morscher and J.A. DiCarlo, "A Simple Test for Thermomechanical Evaluation of Ceramic Fibers," J. Am. Ceram. Soc., 75 [1] 136-140 (1992).
16. ASTM Test Method D3379-75, "Standard Test Method for Tensile Strength and Young's Modulus for High-Modulus Single-Filament Materials," pp. 131-134, Section 15, Vol. 15.03 in 1993 Annual Book of ASTM Standards, Section 15, Vol. 15.03, American Society for Testing and Materials, Philadelphia, PA, 1993.
17. ASTM Test Method D3800-79, Procedure B, "Standard Test Method for Density of High-Modulus Fibers," pp. 172-176, Section 15, Vol. 15.03 in 1988 Annual Book of ASTM Standards, American Society for Testing and Materials, Philadelphia, PA, 1988.
18. E. Serrano and M.D. Sacks, unpublished work.
19. G. Chollon, R. Pailler, R. Naslain, and P. Olry, "Structure, Composition, and Mechanical Behavior at High Temperature of the Oxygen-Free Hi-Nicalon Fiber," pp. 299-302 in *High-Temperature Ceramic-Matrix Composites II: Manufacturing and Materials Development*, Ceram. Trans., Vol. 59. Edited by A.G. Evans and R. Naslain. American Ceramic Society, Westerville, OH, 1995.
20. G.A. Staab and M.D. Sacks, unpublished work
21. T. Mah, N.L. Hecht, D.E. McCullum, J.R. Hoenigman, H.M. Kim, A.P. Katz, H. Lipsitt, "Thermal Stability of SiC Fibres (Nicalon)," J. Mater. Sci., 19 [4] 1191-1201 (1984).
22. G. Simon and A.R. Bunsell, "Mechanical and Structural Characterization of the Nicalon Silicon Carbide Fibre," J. Mater. Sci., 19 [11] 3649-3657 (1984).
23. T.J. Clark, R.M. Arons, J.B. Stamatoff, and J. Rabe, "Thermal Degradation of Nicalon SiC Fiber," Ceram. Eng. Sci. Proc., 6 [7-8] 576-578 (1985).
24. M.H. Jaskowiak and J.A. DiCarlo, "Pressure Effects on the Thermal Stability of Silicon Carbide Fibers," J. Am. Ceram. Soc., 72 [2] 192-197 (1989).
25. R. Bodet, X. Bourrat, J. Lamon, and R. Naslain, "Tensile Creep Behavior of Silicon Carbide-Based Fibre with a Low Oxygen Content," J. Mater. Sci., 30 661-677 (1995).
26. H.M. Yun, J.C. Goldsby, and J.A. DiCarlo, "Environmental Effects on Creep and Stress-Rupture Properties of Advanced SiC Fibers," pp. 331-336 in *High-Temperature Ceramic-Matrix Composites II: Manufacturing and Materials Development*, Ceram. Trans., Vol. 59. Edited by A.G. Evans and R. Naslain. American Ceramic Society, Westerville, OH, 1995.
27. J.A. DiCarlo, Composites Sci. Technol., "Creep Limitations of Current Polycrystalline Ceramic Fibers," 51 213-222 (1994).
28. G.N. Morscher and J.A. Dicarlo, "Creep Resistance of Advanced SiC Fibers," Proceedings of the NASA 6th Annual HITEMP Review, Cleveland, OH, 1993.
29. G.N. Morscher, unpublished results.
30. F. Frechette, B. Dover, V. Venkateswaran, and J. Kim, "High Temperature Continuous Sintered SiC Fiber for Composite Applications," Ceram. Eng. Sci. Proc., 12 [7-8] 992-1006 (1991).

Presented at the conference "New Developments in High Temperature Ceramics," Istanbul, Turkey, August 12-15, 1998. To be published in J. Eur. Ceram. Soc., 1999.

EFFECT OF COMPOSITION AND HEAT TREATMENT CONDITIONS ON THE TENSILE STRENGTH AND CREEP RESISTANCE OF SIC-BASED FIBERS

Michael D. Sacks
Department of Materials Science and Engineering
University of Florida, Gainesville, FL 32611

Abstract

Polymer-derived SiC-based fibers with fine-diameter ($\sim$ 10-15 μm) and high strength ($\sim$ 3 GPa) were prepared with carbon-rich and near-stoichiometric compositions. Fiber tensile strengths were determined after heat treatments at temperatures up to 1950°C in non-oxidizing atmospheres and up to 1250°C in air. The creep resistance of fibers was assessed using bend stress relaxation (BSR) measurements. Fibers showed excellent strength retention after heat treatments in non-oxidizing atmospheres at temperatures up to 1700°C for the carbon-rich fibers and up to 1950°C for the near-stoichiometric fibers. The near-stoichiometric fibers also showed considerably better strength retention after heat treatments in air. Creep resistance of the as-fabricated fibers was greatly improved by high-temperature heat treatments. Heat-treated near-stoichiometric fibers could be prepared with $\sim$ 3 GPa tensile strengths and BSR creep behavior which was significantly better than that reported for Hi-Nicalon™ Type S fibers.

INTRODUCTION

Yajima et al. were the first to demonstrate that organosilicon polymers could be used to fabricate fine-diameter SiC-based fibers with high tensile strength.[1,2] Nicalon™ and Tyranno™ fibers were the first generation of commercially-available polymer-derived fibers which were based on the methods of Yajima et al. However, these fibers are not pure stoichiometric SiC and they contain relatively high concentrations of excess carbon and oxygen. (In addition, Tyranno™ fibers are actually Si-Ti-C-O fibers.) As a consequence, these fibers degrade extensively at high temperatures due to carbothermal reduction reactions between the carbon and siliceous materials.[3-6] To minimize this problem, there has been considerable effort in recent years to prepare organosilicon polymer-derived fibers with low oxygen content.[7-20] Fibers with both carbon-rich and near-stoichiometric compositions have been reported by various researchers, including those at Nippon Carbon Co. (Hi-Nicalon™ and Hi-Nicalon™ Type S fibers)[7-12], Dow Corning Co. (Sylramic™ fibers)[13-16], and the University of Florida (UF and UF-HM fibers).[17-20] These fibers show significantly improved thermomechanical properties compared to fibers containing large amounts of oxygen, such as Nicalon™ and Tyranno™ fibers.

In this study, the tensile strength of both carbon-rich fibers and near-stoichiometric fibers were determined before and after heat treatments in oxidizing and non-oxidizing atmospheres. The creep resistance of these fibers was assessed under inert-atmosphere heat-treatment conditions using the bend stress relaxation (BSR) method of Morscher and DiCarlo.[21]

EXPERIMENTAL

Processing

Carbon-rich fibers and near-stoichiometric SiC-based fibers were fabricated using a high-molecular-weight polycarbosilane (PCS) polymer as the primary ceramic precursor.[17-20] The infusible PCS polymers were prepared by pressure pyrolysis of polydimethylsilane.[18] Fine-diameter ($\sim$ 10-15 μm) fibers were formed by dry spinning of concentrated PCS-based polymer solutions.[18] The as-spun polymeric fibers were dried and subsequently given different heat treatments depending on the desired composition. Carbon-rich fibers (designated "UF fibers") were prepared by directly pyrolyzing the dried fibers at temperatures in the range of $\sim$1000-

1200°C in a non-oxidizing atmosphere (e.g., nitrogen). Fibers with near-stoichiometric composition were produced by carrying out controlled carbothermal reduction reactions at elevated temperatures. After drying, the spun polymeric fibers were initially heat treated in air or oxygen at low temperatures ($\sim$100-200°C) to incorporate oxygen into the organosilicon polymer. The fibers were then heat treated in inert atmosphere (e.g., argon) to decompose the oxidized organosilicon polymer to an $SiC/C/SiC_xO_y$ ceramic (at $<$1200°C) and to subsequently effect the carbothermal reduction reductions (at $\sim$1400-1600°C) in which excess carbon was eliminated from the fiber by reaction with siliceous phase. This resulted in near-stoichiometric microporous SiC fibers which were subsequently sintered (at $\geq$1750°C) in inert atmosphere. Boron additions (typically $\sim$1 wt%) were used as a sintering aid.

Characterization

Several techniques were used to characterize fiber composition, microstructure, and properties. Quantitative bulk elemental analyses were carried out on individual fibers using an electron microprobe analyzer, EMA (Superprobe 733 Scanning Electron Microprobe, JEOL, Tokyo, Japan) equipped with X-ray wavelength dispersive spectrometers. High purity single-crystal silicon, CVD silicon carbide, silicon dioxide, and silicon nitride (all from Geller Microanalytical Laboratory, Peabody, MA) were used as measurement standards for Si, C, O, and N analyses, respectively. Bulk oxygen concentrations were also determined by neutron activation analysis, NAA, (Nicolet Electron Services, San Diego, CA). NAA was also used to determine bulk boron concentrations (University of Missouri Research Reactor, Columbia, MO). Compositional analyses of the near-surface region of individual fibers was carried out using a scanning Auger microprobe, SAM (model PHI 660, Perkin Elmer Corp., Eden Prairie, MN).

SEM (Model JSM-6400, JEOL) and TEM (Models 200CX and 4000FX, JEOL) were used to characterize the fiber microstructural features, including the external surface morphology, phases present, grain sizes, porosity, and flaw sizes determined from the fracture surfaces of individual fibers collected after tensile tests. The constituent phases of the fibers were identified using electron diffraction, high resolution TEM, and X-ray diffraction, XRD (Model APD 3720, Philips Electronics Instrument Co., Mt. Vernon, NY).

Fiber apparent densities were determined at 23°C by a sink-float method (ASTM procedure D3800-79).[22] The liquids used were methylene iodide (CH_2I_2, density ~3.3 g/mL) and carbon tetrachloride (CCl_4, density ~1.6 g/mL).

Fiber tensile strengths were determined at room temperature according to ASTM procedure D3379.[23] Individual fibers were glued to paper tabs and loaded in tension (0.5 mm/min cross-head speed) until failure using a mechanical testing apparatus (Model 1122, Instron Corp. Canton MA). The gage length was 25 mm. Fiber diameters were determined prior to testing using an optical microscope equipped with a micrometer in the eyepiece.

The creep behavior of fibers was assessed using the bend stress relaxation (BSR) method of Morscher and DiCarlo.[21] In this method, stress relaxation values (designated as "M" values) are determined based on the extent of permanent deformation that occurs when fibers are heat treated under an applied bending load. An M value which approaches 1 indicates that no permanent (creep) deformation occurred during the high temperature annealing, while an M value of 0 indicates that the stress completely relaxed. Hence, fibers are considered more thermally stable against creep as the M values increase from 0 to 1. The BSR tests were carried out using heat treatments at temperatures in the range of 1100-1850°C for 1 h in an argon atmosphere.

RESULTS AND DISCUSSION

As-Fabricated Fibers

Fibers with Carbon-Rich Compositions

The normalized Si/C weight ratios for the as-pyrolyzed (<1200°C) UF fibers were in the range of ~59-62 wt% Si/38-41 wt% C, with an average ratio (determined from 8 samples) of ~60.5 wt% Si/~39.5 wt% C. Hence, these fibers were highly carbon-rich compared to stoichiometric SiC (~70 wt% Si/~30 wt% C). Some oxygen impurity was incorporated in the fiber during the various stages of processing,[18] but the concentrations for the fibers used in this study were limited to ~0.5-1.0 wt%. Some of the fibers were also doped with small amounts of boron (<1 wt%). The phases present in the UF fibers were β-SiC and XRD-amorphous

on. TEM and XRD line-broadening measurements indicated that the β-SiC crystallite sizes ≤ 5 nm. Sink-float measurements showed that the fiber apparent densities were in the of $\sim 2.5\text{-}2.7$ g/cm^3. The relatively low densities are consistent with the presence of excess on in the fibers and the weakly crystalline nature of the SiC grains. (In contrast, well-ystallized, high-purity SiC has a density of ~ 3.21 g/cm^3.)

Figure 1 shows histogram plots of the average room temperature tensile strengths and average diameters obtained from 43 separate sets of the UF fibers. (In most cases, ≥ 15 fibers were tested for each set.) The mean tensile strength was 3.23 GPa (468 ksi). The mean diameter for these test sets was 12.6 μm.

Figure 2 shows a plot of the fiber tensile strength vs. the flaw size measured from the fracture surfaces of tested UF fibers. Although there is considerable scatter in the data, high-strength fibers (e.g., ~ 3 GPa) typically have flaws in the range of $\sim 0.2\text{-}0.3$ μm. This corresponds closely to the smallest pore sizes of the filters (nominal sizes were 0.1-0.2 μm) that were used to prepare the spinning solutions for fiber fabrication. In previous work [18], it was observed that fibers had lower average tensile strength when the spinning solutions were prepared using filters with coarser pore sizes. Hence, it is suggested that the tensile strength of the UF fibers is controlled primarily by processing-related particulates (i.e., impurity particles, polymer "microgel" particles, etc.) that remain in the spin dope after filtration.

Fibers with Near-Stoichiometric Composition

The normalized Si/C weight ratios for the as-sintered, near-stoichiometric UF-HM fibers were mostly in the range of $\sim 67\text{-}70$ wt% Si/30-33 wt% C, with an average composition (determined from >25 samples) of ~ 68.5 wt% Si/~ 31.5 wt% C. This indicates that the fibers typically contained a small amount of excess carbon. Residual carbon was not detected by a standard X-ray powder diffraction method, but was observed by TEM. HRTEM analysis showed the stacked hexagonal structural units with interplanar spacing of 0.34 nm that are associated with graphitic carbon. X-ray and electron diffraction analyses showed that β-SiC was the primary phase in the UF-HM fibers, although traces of the alpha phase were present in some fibers (based on electron diffraction results). EMA analysis for oxygen and nitrogen showed that

concentrations were less than the resolution limit for the technique (typically ≤ 0.2 wt%). The boron concentrations were usually on the order of 1 wt%, although it was possible to prepare fibers with range of boron concentrations (i.e., ~ 0.1 - 3.0 wt%).

The apparent densities of the UF-HM fibers were usually in the range of 3.1-3.2 g/cm^3, with an average value of ~ 3.15 g/cm^3. The average density is lower than the theoretical value (of 3.21 g/cm^3) for fully dense (pore-free), stoichiometric SiC. This is attributed, in part, to the small amount of residual carbon in the fibers. In addition, TEM showed that a small amount of fine pores (usually less than 0.1 μm) was present at some grain junctions.

Figure 3 shows histogram plots of the average room temperature tensile strengths and average diameters obtained for 150 separate sets of as-sintered UF-HM fibers. (In most cases, ≥ 15 fibers were tested for each set.) The mean tensile strength was 2.85 GPa (413 ksi). The mean diameter for these test sets was 12.1 μm. A detailed fractographic analysis was not carried out for the UF-HM fibers, but it is believed that the tensile strengths were controlled mostly by larger grains at the fiber surface. Although most of the grains were generally in the range of ~ 0.05 - 0.3 μm, grains as large as ~ 0.5-1.0 μm were observed occasionally (see Fig. 4).

Effect of Heat Treatments on Fiber Tensile Strength and BSR Creep Resistance

Fibers with Carbon-Rich Compositions

Figure 5 shows room temperature tensile strengths for UF fibers after heat treatments in argon for 1 h at temperatures in the range of 1500-1900°C. There was no loss in strength with heat treatments up to 1700°C and then the strength decreased rapidly with further heat treatments up to 1900°C. Fig. 5 also shows that the UF fibers have greater retention of their original strengths after high temperature (e.g., ≥ 1600°C) heat treatments in argon compared to the strength retention reported for carbon-rich Hi-Nicalon™ fibers.[10,11,24]

For Hi-Nicalon™ fibers, strength decreases upon heat treatment in inert atmospheres have been attributed to a combination of coarsening of SiC grains and flaw formation resulting from thermochemical degradation reactions.[24] SEM observations of the fracture surfaces of the UF fibers heat treated at 1700°C and 1900°C did not reveal any obvious differences in the flaw

populations. TEM observations (Figure 6) did show that the SiC grains coarsened with increasing heat treatment temperature. However, even after heat treatment at 1900°C for 1 h in argon, the grains are still relatively small (e.g., compared to the high-strength UF-HM fibers shown in Fig. 4). Hence, it is unlikely that coarser grains act directly as strength-controlling flaws responsible for the lower strength in the 1900°C heat-treated UF fibers.

A possible explanation for the rapid decrease in strength for the 1900°C heat-treated fibers is the presence of residual tensile stresses at the fiber surface. Residual tensile stresses might develop as a result of the mismatch in thermal expansion coefficients between SiC and C. These stresses would become larger as the SiC/C structure coarsens during heat treatment at higher temperatures. Figure 6 shows that both the β-SiC grains and the carbon regions grow to larger size with increasing heat treatment temperature. It is also known that the carbon-rich regions in PCS-derived SiC fibers become more highly ordered (i.e., more graphitic) as fibers are heat treated above the original fabrication temperature.[24,25] This is significant because graphite has a very large difference in the thermal expansion coefficients for the directions parallel and normal to the hexagonal basal planes and, hence, higher thermal expansion mismatch stresses might be expected.

It is not understood why the UF fibers show improved strength retention upon heat treatment in argon compared to the Hi-Nicalon™ fibers. The fibers have similar chemical and phase compositions and similar grain sizes. The differences in strength retention could be due to minor differences in impurities in the fibers. For example, it has been observed that strength retention is highly sensitive to low levels of oxygen impurities.[8,18] In addition, the purity of the atmosphere and the presence of contaminants during the heat treatments of the fibers can have a significant effect on the strength retention of these fibers. (For example, oxygen impurities in an otherwise inert heat treatment atmosphere have been observed to cause significant decreases in the fiber strength.)

Figure 7 shows plots of the bend stress relaxation ratios, M, as a function of the heat treatment temperature for as-pyrolyzed (1200°C) UF fibers and for UF fibers which were given heat treatments for 1 h (in argon) at 1700°C and 1900°C. Heat treatment of the UF fibers results in improved BSR creep resistance. This is consistent with reports from other researchers that

Hi-Nicalon™ and Hi-Nicalon™ Type S fibers become more creep-resistant after annealing heat treatments above the original processing temperature.[12,26] This may be attributed to the increased grain sizes and/or the more highly crystallized graphitic carbon. Both microstructural changes are expected to inhibit diffusion-controlled creep processes.

Figure 7 also shows the BSR data that has been reported [12,27-29] for Hi-Nicalon™ and Hi-Nicalon™ Type S fibers. The Hi-Nicalon™ fibers have somewhat higher M values (for a given BSR test temperature) compared to the as-prepared UF fibers. This is attributed to a slightly higher initial processing temperature for the Hi-Nicalon™ fibers which, in turn, results in slightly coarser microstructures (including larger SiC crystallite sizes). The Hi-Nicalon™ Type S fiber have significantly higher M values (for a given BSR test temperature) compared to the Hi-Nicalon™ fibers and the as-pyrolyzed UF fibers. This is attributed to the much larger grain sizes of the Hi-Nicalon™ Type S fiber.[12]

The 1700°C heat-treated UF fibers not only show greatly improved creep resistance, but also retain high tensile strength. The creep resistance of these fibers (based on the BSR test results) is comparable to or better than the Hi-Nicalon™ Type S fibers. This occurs despite the fact that the grain sizes are much larger for the latter fibers.[12] This observations again indicates that diffusion is inhibited in SiC-based fibers with larger amounts of excess carbon. This manifests itself not only in the slower coarsening of SiC grains upon heat treatment (as indicated by comparing the grain sizes in Figs. 4 and 6 for carbon-rich and near-stoichiometric fibers), but also in the improved creep resistance of the fibers.

As-pyrolyzed UF fibers and UF fibers heat treated in argon at 1650°C were subsequently given heat treatments in air for 1 h at temperatures in the range of 500-1150°C. Figure 8 shows the room temperature tensile strengths for these fibers after the air heat treatments. The decreases in strength are attributed to the formation of porosity (and possibly other flaws) resulting from the oxidative combustion of the carbon phase in the fibers. As noted from Fig. 6, the SiC/C fiber microstructure coarsens significantly during the argon annealing heat treatment. The coarser microstructure in the 1650°C fibers evidently allows oxygen to react with the carbon phase more readily. The fiber strength begins to decrease in the range of only 500-600°C, i.e., at similar temperatures for which significant reaction occurs when bulk carbon is

heat treated to air. Figure 8 also shows that the tensile strengths for the 1650°C fibers level off after the 900°C air heat treatment. It is presumed that this correlates with the removal of most of the excess carbon from the fiber. In contrast to these results, the oxidative removal of carbon from the as-pyrolyzed UF fibers occurs at considerably higher temperatures. Strength decreases are not observed until the air heat treatment temperature is greater than ~950°C. This is attributed to the development of a thin siliceous surface layers during air heat treatment which would inhibit oxidative removal of the carbon at the lower temperatures.

Fibers with Near-Stoichiometric Composition

Figure 9 shows a direct comparison of the room temperature tensile strengths for the carbon-rich UF fibers and the near-stoichiometric UF-HM fibers after heat treatments in argon for 1 h at temperatures in the range of 1400-1950°C. The UF-HM fibers retained most of their original strength through heat treatments up to 1800°C and then the strength gradually decreased with heat treatments at higher temperatures (up to 1950°C). As noted earlier, the UF fibers show a relatively rapid decrease in the tensile strength after heat treatments above 1700°C.

The strength-controlling flaws for the as-sintered UF-HM fibers are believed to be larger grains at the fiber surfaces. Hence, the gradual decrease in tensile strength for the UF-HM fibers after heat treatment in argon at higher temperatures is attributed to grain growth. Although quantitative measurements have not been made, TEM observations did show that larger grains were more prevalent in the 1950°C heat-treated fibers compared to the as-sintered fibers.

The near-stoichiometric UF-HM fibers retained most of their initial strength to higher temperature than the carbon-rich UF fibers despite the considerably larger grain sizes of the former fibers. Hence, the relatively rapid decrease in strength in UF fibers heat treated above 1700°C cannot be attributed to larger grains acting directly as strength-controlling flaws. As noted earlier, it is instead believed that the strength decay results from larger residual stresses arising from the mismatch in the SiC/C thermal expansion coefficients.

The UF-HM fibers show even better strength retention when heat treated in nitrogen-containing atmosphere instead of argon. The as-fabricated tensile strengths were retained after heat treatments up to ~1950°C. The reason for this behavior is unclear, but it is believed to

be associated with the formation of a thin BN layer ($\sim$0.1-0.2 μm) on the fiber surface. The BN forms in-situ (i.e., during heat treatment) by the reaction of boron that is initially present in the fiber (as a sintering aid) and nitrogen in the annealing atmosphere.[30] The improved strength retention is believed to result from restricting the flaw size at the fiber surface to the approximate thickness of the BN layer.

Figure 10 shows BSR data for the as-sintered and nitrogen-annealed UF-HM fibers. Annealing results in significant improvements in creep resistance. In fact, the annealed fibers show comparable BSR behavior to that reported [27-29] for much weaker, coarse-grained Carborundum fibers. (The latter fibers were prepared by sintering of SiC powders and have considerably larger grain sizes, larger diameters, and rougher surfaces compared to typical polymer-derived SiC fibers.[31] The coarser grain sizes results in fibers which have excellent creep resistance, but relatively low tensile strength.) The improved creep resistance of the UF-HM fibers after the annealing treatment is attributed, at least in part, to increased grain sizes. It is also possible that boron removal from the bulk of the fiber (i.e., due to migration to the fiber surface) decreases SiC self-diffusion coefficients and thereby decreases the creep rate.

Takeda et al.[12] reported that annealing heat treatments improved the creep resistance of Hi-Nicalon™ Type S fibers. However, these fibers did not retain tensile strengths as high as the UF-HM fibers after the annealing heat treatments. This is illustrated in Fig. 11 which shows plots of tensile strengths vs. M values for Hi-Nicalon™ Type S and UF-HM fibers which were subjected to various annealing heat treatments prior to BSR tests at 1400°C (for 1 h argon). UF-HM fibers could be prepared which had 1400°C BSR M values of $\sim$0.9, while still retaining tensile strengths of $\sim$3 GPa. In contrast, 1400°C BSR M values of only $\sim$0.6 were possible in Hi-Nicalon™ Type S fibers which retained tensile strengths of $\sim$3 GPa.

Figure 12 shows the room temperature tensile strengths for as-sintered UF-HM fibers after they were heat treated in air for 1 h at temperatures in the range of 400-1250°C. The fibers show excellent strength retention under these heat treatment conditions. The curve drawn in Fig. 12 suggests that there is a small initial decrease in strength as the heat treatment temperature is increased from 500 to 600°C and another small decrease in strength after heat treatment at 1250°C. It could be argued that the differences in strength values for various points

in Fig. 12 are not statistically significant since all the values are within ±1 standard on of the average value. However, the trends suggested for the curve drawn in Fig. 10 pported by other observations: (1) Scanning auger microprobe (SAM) measurements that heat treatment in air above 500°C removes a thin (typically ~10-20 nm) carbon-rich yer from the UF-HM fiber surfaces. (It is well-known that Si tends to evaporate preferentially from the surface of SiC during high temperature heat treatment in inert or vacuum atmospheres. SAM measurements showed that the as-sintered UF-HM fibers have a thin carbon layer on the surface.) The oxidative elimination of the carbon surface layer may lead to increased concentration and/or size of surface flaws. (2) The fibers are expected to develop thicker silica surface layers as the oxidation temperature increases. After the 1250°C heat treatment in air, it was evident that the individual fibers were beginning to stick together (i.e., presumably due to viscous flow of the silica surface layers). It is likely that surface damage was introduced when these fibers were separated for the tensile tests.

CONCLUSIONS

Carbon-rich and near-stoichiometric SiC fibers with fine-diameter (~10-15 μm) and high tensile strength (~3 GPa) were prepared by dry spinning of polycarbosilane-based polymer solutions. The effects of heat treatments in oxidizing and non-oxidizing atmospheres on the thermomechanical properties of carbon-rich and near-stoichiometric SiC fibers were investigated.

The carbon-rich UF fibers showed excellent strength retention after heat treatments in argon (1 hr) up to 1700°C and then showed relatively sharp decreases in strength. The strength decrease at higher temperatures was attributed to increasing residual stresses arising from mismatches in the thermal expansion coefficients in the SiC/C fibers. The near-stoichiometric UF-HM fibers showed excellent strength retention after heat treatments in argon (1 h) up to 1800°C and then showed a relatively gradual decrease in strength. The strength decrease was attributed to increased grain sizes as a result of grain growth. The near-stoichiometric fibers were able to retain their initial tensile strengths to even higher temperature (1950°C) when heat treatments were carried in nitrogen. This observation was associated with the formation of a thin BN layer (~0.1-0.2 μm) at the fiber surface which was believed to restrict the size of the

strength-degrading flaws at the fiber surface.

The as-prepared carbon-rich UF fibers showed significant improvements in creep resistance (as assessed by the bend stress relaxation, BSR, method) when heat treated at elevated temperatures in argon. This was attributed to the increased grain sizes and possibly more highly crystallized graphitic carbon. Despite finer SiC grain sizes, the carbon-rich UF fibers heat treated at 1700°C in argon showed creep resistance (based on the BSR test results) which was comparable to or better than that observed for the as-prepared near-stoichiometric fibers (both UF-HM fibers and Hi-Nicalon™ Type S fibers). This result indicated that diffusion is inhibited in SiC-based fibers which contain larger amounts of excess carbon. The BSR creep resistance of the near-stoichiometric UF-HM fibers was also enhanced significantly by annealing heat treatments in nitrogen. This was attributed to increased grain size and reduced boron concentration within the bulk fiber.

UF-HM fibers showed excellent strength retention after heat treatment in air (1 h) at temperatures in the range of 400-1150°C. Interfilament adhesion occurred when the fiber bundles were heat treated at 1250°C, presumably due to viscous flow of siliceous material that had formed at the fiber surface. Strengths decreased after heat treatments in air at much lower temperatures for the carbon-rich UF fibers compared to the near-stoichiometric UF-HM fibers. This was attributed to formation of porosity (and possibly other flaws) when carbon was oxidatively eliminated from the UF fibers. The strength decreases in the carbon-rich fibers occurred at substantially lower temperature for the 1650°C argon heat-treated fibers compared to the as-pyrolyzed fibers. This was attributed to an enhanced oxidative attack of the carbon due to the considerably coarser SiC/C microstructure of the 1650°C fibers.

ACKNOWLEDGMENT

The author thank J.A. DiCarlo and G.N. Morscher of the NASA Lewis Research Center for assistance with the BSR measurements and helpful discussions; W. Coblenz of DARPA for helpful discussions; G.W. Scheiffele, G.A. Staab, M. Saleem, G. Brubaker, A.A. Morrone, E. Serrano, L. Zhang, T.J. Williams, and Y. Yang of the University of Florida for experimental contributions; and D. Kutikkad of the University of Missouri for the boron analysis by NAA. Support for this work by the Advanced Research Projects Agency and the Office of Naval Research (N00014-91-J-4075, N00014-93-1-0853), Air Force Office of Scientific Research, (F49620-94-1-0429, F49620-97-1-0095), and the IHPTET Fiber Development Consortium (IHP-UFLA-93A374-005, IHP-MMM-96A374-011) is gratefully acknowledged.

REFERENCES

1. S. Yajima, J. Hayashi, M. Omori, and K. Okamura, "Development of a Silicon Carbide Fiber with High Tensile Strength," Nature, 261 683-685 (1976).
2. S. Yajima, K. Okamura, J. Hayashi, and M. Omori, "Synthesis of Continuous SiC Fibers with High Tensile Strength," J. Am. Ceram. Soc., 59 324-327 (1976).
3. T. Mah, N.L. Hecht, D.E. McCullum, J.R. Hoenigman, H.M. Kim, A.P. Katz, H. Lipsitt, J. Mater. Sci., **19**(4), 1191-1201 (1984).
4. G. Simon and A.R. Bunsell, J. Mater. Sci., **19**(11), 3649-3657 (1984).
5. T.J. Clark, R.M. Arons, J.B. Stamatoff, and J. Rabe, Ceram. Eng. Sci. Proc., **6**(7-8), 576-578 (1985).
6. M.H. Jaskowiak and J.A. DiCarlo, J. Am. Ceram. Soc., **72**(2), 192-197 (1989).
7. M. Takeda, Y. Imai, H. Ichikawa, and T. Ishikawa, "Properties of the Low Oxygen Content SiC Fiber on High Temperature Heat Treatment", Ceram. Eng. Sci. Proc., 12 [7-8] 1007-1018 (1991).
8. M. Takeda, Y. Imai, H. Ichikawa, T. Ishikawa, N. Kasai, T. Suguchi, and K. Okamura "Thermal Stability of the Low Oxygen Content Silicon Carbide Fibers Derived from Polycarbosilane," Ceram. Eng. Sci. Proc., 13 [7-8] 209-217 (1992).
9. T. Ishikawa, "Recent Developments of the SiC Fiber Nicalon and Its Composites, Including Properties of the SiC Fiber Hi-Nicalon for Ultra-High Temperature," Composites Sci. Technol., 51 135-144 (1994).
10. M. Takeda, J. Sakamoto, Y. Imai, H. Ichikawa, and T. Ishikawa, "Properties of Stoichiometric Silicon Carbide Fiber Derived from Polycarbosilane," Ceram. Eng. Sci. Proc., 15 [4] 133-141 1994.
11. M. Takeda, J. Sakamoto, A. Saeki, Y. Imai, and H. Ichikawa, Ceram. Eng. Sci. Proc., "High Performance Silicon Carbide Fiber Hi-Nicalon for Ceramic Matrix Composites," 16 [4] 37-44 1995.
12. M. Takeda, J. Sakamoto, A. Saeki, and H. Ichikawa, Ceram. Eng. Sci. Proc., "Mechanical and Structural Analysis of Silicon Carbide Fiber Hi-Nicalon Type S," 17 [4] 35-43 1996.
13. J. Lipowitz, J.A. Rabe, and G.A. Zank, "Polycrystalline SiC Fibers from Organosilicon Polymers," Ceram. Eng. Sci. Proc., 12 [9-10] 1819-1831 (1991).
14. Y. Xu, A. Zangvil, J. Lipowitz, J.A. Rabe, and G.A. Zank, "Microstructure and Microchemistry of Polymer-Derived Crystalline SiC Fibers," J. Am. Ceram. Soc., 76 [12] 3034-3040 (1993).
15. J. Lipowitz, T. Barnard, D. Bujalski, J.A. Rabe, G.A. Zank, Y. Xu, and A. Zangvil, "Fine-Diameter Polycrystalline SiC Fibers," Composites Sci. Technol., 51 167-171 (1994).
16. J. Lipowitz, J.A. Rabe, G.A. Zank, A. Zangvil and Y. Xu, "Structure and Properties of Sylramic™ Silicon Carbide Fiber – a Polycrystalline, Stoichiometric β-SiC Composition," Ceram. Eng. Sci. Proc., 18 [3] 147-157 (1997).
17. Wm. Toreki, G.J. Choi, C.D. Batich, M.D. Sacks, and M. Saleem, "Polymer-Derived Silicon Carbide Fibers with Low Oxygen Content," Ceram. Eng. Sci. Proc., 13 [7-8] 198-208 (1992).
18. Wm. Toreki, C.D. Batich, M.D. Sacks, M. Saleem, G.J. Choi, and A.A. Morrone, "Polymer-Derived Silicon Carbide Fibers with Low Oxygen Content and Improved Thermomechanical Stability," Composites Sci. Technol., 51 145-159 (1994).
19. M.D. Sacks, A.A. Morrone, G.W. Scheiffele, and M. Saleem, "Characterization of Polymer-Derived Silicon Carbide Fibers with Low Oxygen Content, Near-Stoichiometric Composition, and Improved Thermomechanical Stability," Ceram. Eng. Sci. Proc., 16 [4] 25-35 (1995).
20. M.D. Sacks, G.W. Scheiffele, M. Saleem, G. Staab, T.J. Williams, and A.A. Morrone, "Polymer-Derived Silicon Carbide Fibers with Near-Stoichiometric Composition and Low Oxygen Content," pp. 3-10 in *Ceramic Matrix Composites - Advanced High Temperature Structural Materials*, Mat. Res. Soc. Symp. Proc., Vol. 365. Edited by R.A. Lowden, M.K. Ferber, J.R. Hellmann, S.G. DiPietro, and K.K. Chawla. Materials Research Society, Pittsburgh, PA, 1995.

21. G.N. Morscher and J.A. DiCarlo, "A Simple Test for Thermomechanical Evaluation of Ceramic Fibers," J. Am. Ceram. Soc., 75 [1] 136-140 (1992).
22. ASTM Test Method D3800-79, Procedure B, "Standard Test Method for Density of High-Modulus Fibers," pp. 172-176, Section 15, Vol. 15.03 in 1988 Annual Book of ASTM Standards, American Society for Testing and Materials, Philadelphia, PA, 1988.
23. ASTM Test Method D3379-75, "Standard Test Method for Tensile Strength and Young's Modulus for High-Modulus Single-Filament Materials," pp. 131-134, Section 15, Vol. 15.03 in 1993 Annual Book of ASTM Standards, Section 15, Vol. 15.03, American Society for Testing and Materials, Philadelphia, PA, 1993.
24. G. Chollon, R. Pailler, R. Naslain, and P. Olry, "Structure, Composition, and Mechanical Behavior at High Temperature of the Oxygen-Free Hi-Nicalon Fiber," pp. 299-302 in *High-Temperature Ceramic-Matrix Composites II: Manufacturing and Materials Development*, Ceram. Trans., Vol. 59. Edited by A.G. Evans and R. Naslain. American Ceramic Society, Westerville, OH, 1995.
25. R. Bodet, X. Bourrat, J. Lamon, and R. Naslain, "Tensile Creep Behavior of Silicon Carbide-Based Fibre with a Low Oxygen Content," J. Mater. Sci., 30 661-677 (1995).
26. H.M. Yun, J.C. Goldsby, and J.A. DiCarlo, "Environmental Effects on Creep and Stress-Rupture Properties of Advanced SiC Fibers," pp. 331-336 in *High-Temperature Ceramic-Matrix Composites II: Manufacturing and Materials Development*, Ceram. Trans., Vol. 59. Edited by A.G. Evans and R. Naslain. American Ceramic Society, Westerville, OH, 1995.
27. J.A. DiCarlo, Composites Sci. Technol., "Creep Limitations of Current Polycrystalline Ceramic Fibers," 51 213-222 (1994).
28. G.N. Morscher and J.A. DiCarlo, "Creep Resistance of Advanced SiC Fibers," Proceedings of the NASA 6th Annual HITEMP Review, Cleveland, OH, 1993.
29. G.N. Morscher, private communication/unpublished results.
30. M.D. Sacks, G.W. Scheiffele, L. Zhang, Y. Yang, J.J. Brennan, "Polymer-Derived SiC-Based Fibers with High Tensile Strength and Improved Creep Resistance," to be published in Ceram. Eng. Sci., Proc., 19 (1998).
31. F. Frechette, B. Dover, V. Venkateswaran, and J. Kim, "High Temperature Continuous Sintered SiC Fiber for Composite Applications," Ceram. Eng. Sci. Proc., 12 [7-8] 992-1006 (1991).

FIGURE CAPTIONS

Figure 1. Histogram plots of frequency vs. average tensile strength and frequency vs. average diameter for 43 sets of carbon-rich UF fibers.

Figure 2. Plot of tensile strength vs. flaw size for individually tested UF fibers.

Figure 3. Histogram plots of frequency vs. average tensile strength and frequency vs. average diameter for 150 sets of near-stoichiometric UF-HM fibers.

Figure 4. TEM micrographs showing the grains in a near-stoichiometric UF-HM fiber.

Figure 5. Plot of average tensile strength vs. heat treatment temperature (in argon for 1 h) for carbon-rich UF fibers. Data reported by other researchers for Hi-Nicalon™ fibers are also shown.

Figure 6. TEM micrographs for as-pyrolyzed carbon-rich UF fibers (1200°C) and for UF fibers heat treated in argon for 1 h at 1700°C and 1900°C.

Figure 7. Plots of stress relaxation ratio, M, vs. heat treatment temperature for as-pyrolyzed carbon-rich UF fibers (1200°C), argon heat-treated (1700°C and 1900°C) UF fibers, Hi-Nicalon™ fibers, and Hi-Nicalon™ Type S fibers.

Figure 8. Plots of average tensile strength vs. heat treatment temperature (in air for 1 h) for as-pyrolyzed carbon-rich UF fibers and for argon heat-treated (1650°C) UF fibers.

Figure 9. Plots of average tensile strength vs. heat treatment temperature (in argon for 1 h) for carbon-rich UF fibers and near-stoichiometric UF-HM fibers.

Figure 10. Plots of stress relaxation ratio, M, vs. heat treatment temperature for as-sintered near-stoichiometric UF-HM fibers, heat-treated UF-HM fibers, and Carborundum fibers.

Figure 11. Plots of tensile strength vs. stress relaxation ratio, M, for near-stoichiometric UF-HM fibers and Hi-Nicalon Type S fibers which were given varying annealing treatments in order to alter the M values. The BSR tests were carried out at 1400°C.

Figure 12. Plot of average tensile strength vs. heat treatment temperature (in air for 1 h) for near-stoichiometric UF-HM fibers.

Figure 1

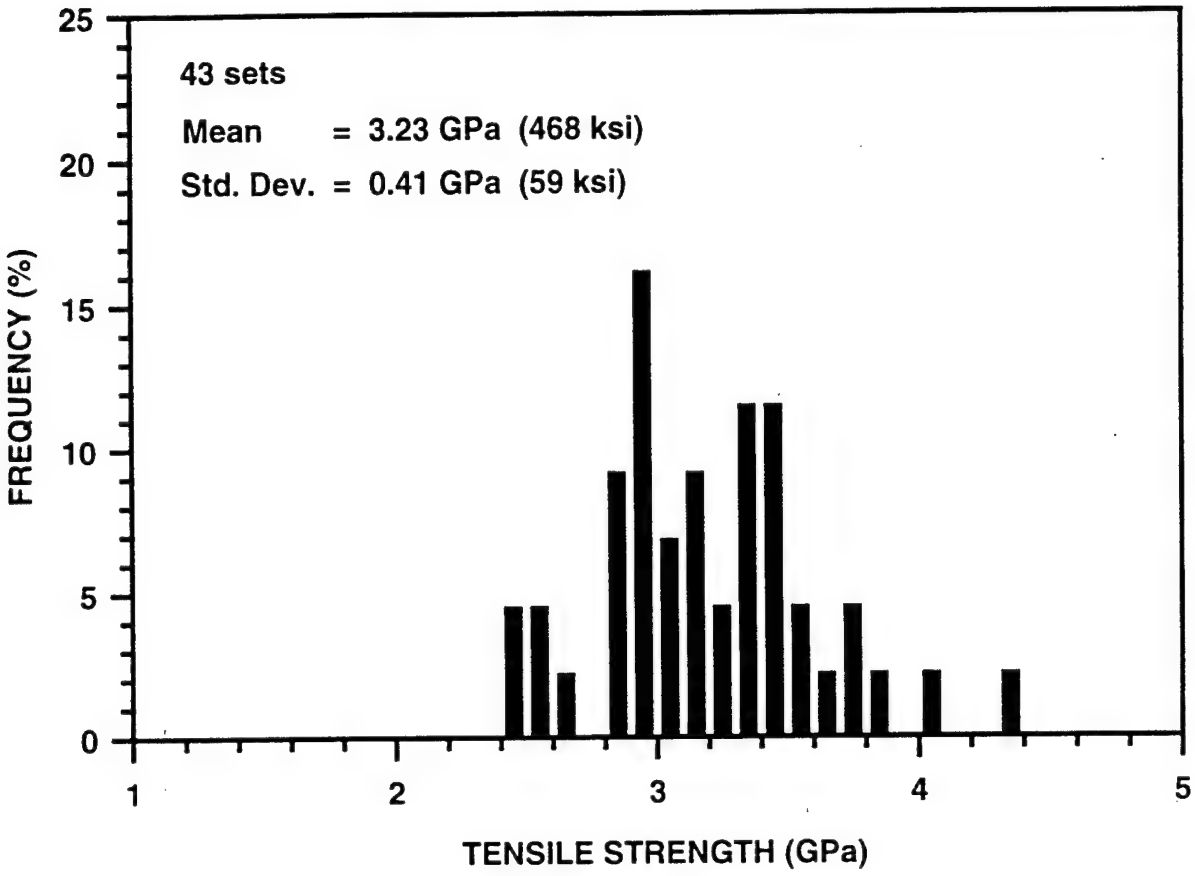
43 sets
Mean = 3.23 GPa (468 ksi)
Std. Dev. = 0.41 GPa (59 ksi)
FREQUENCY (%)
0
5
10
15
20
25
1
2
3
4
5
TENSILE STRENGTH (GPa)

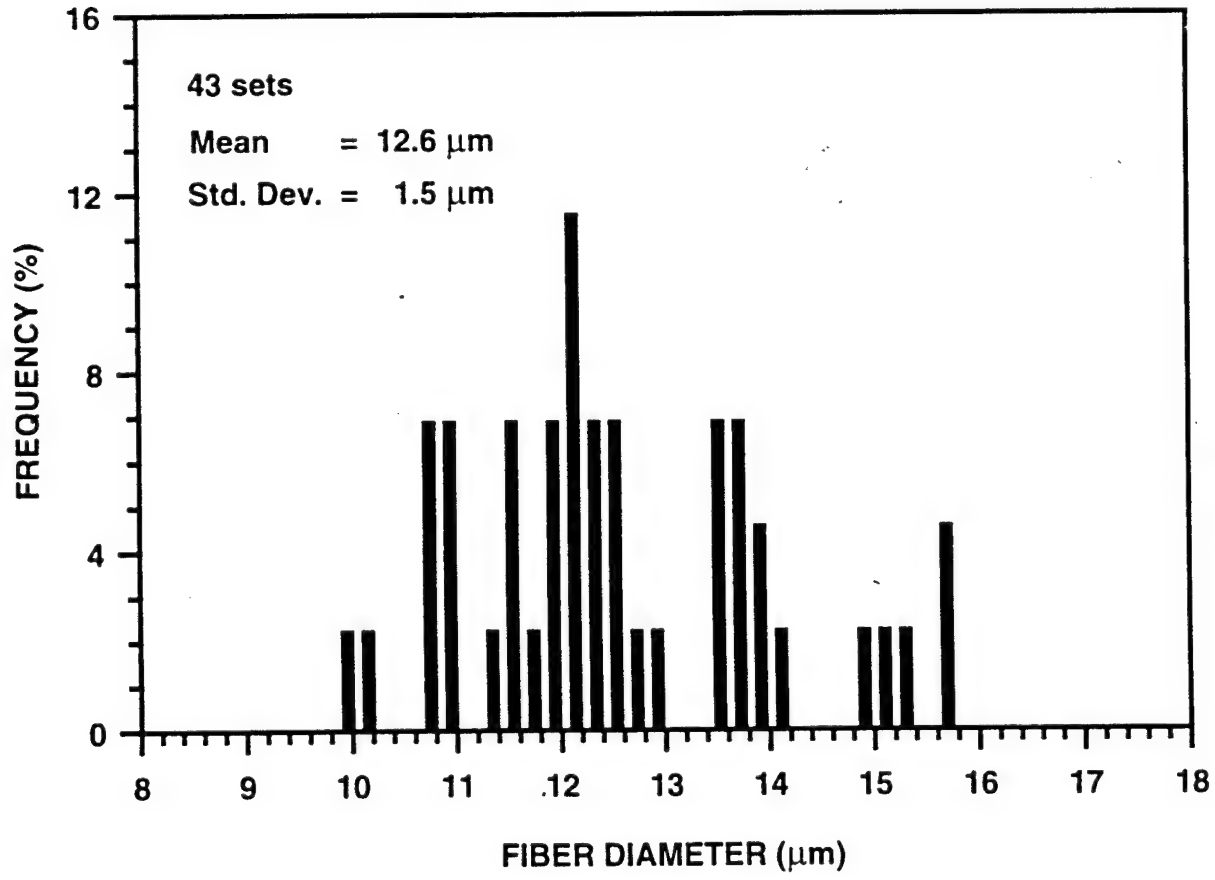
43 sets
Mean = 12.6 μm
Std. Dev. = 1.5 μm
FREQUENCY (%)
0
4
8
12
16
8
9
10
11
12
13
14
15
16
17
18
FIBER DIAMETER (μm)

Figure 2

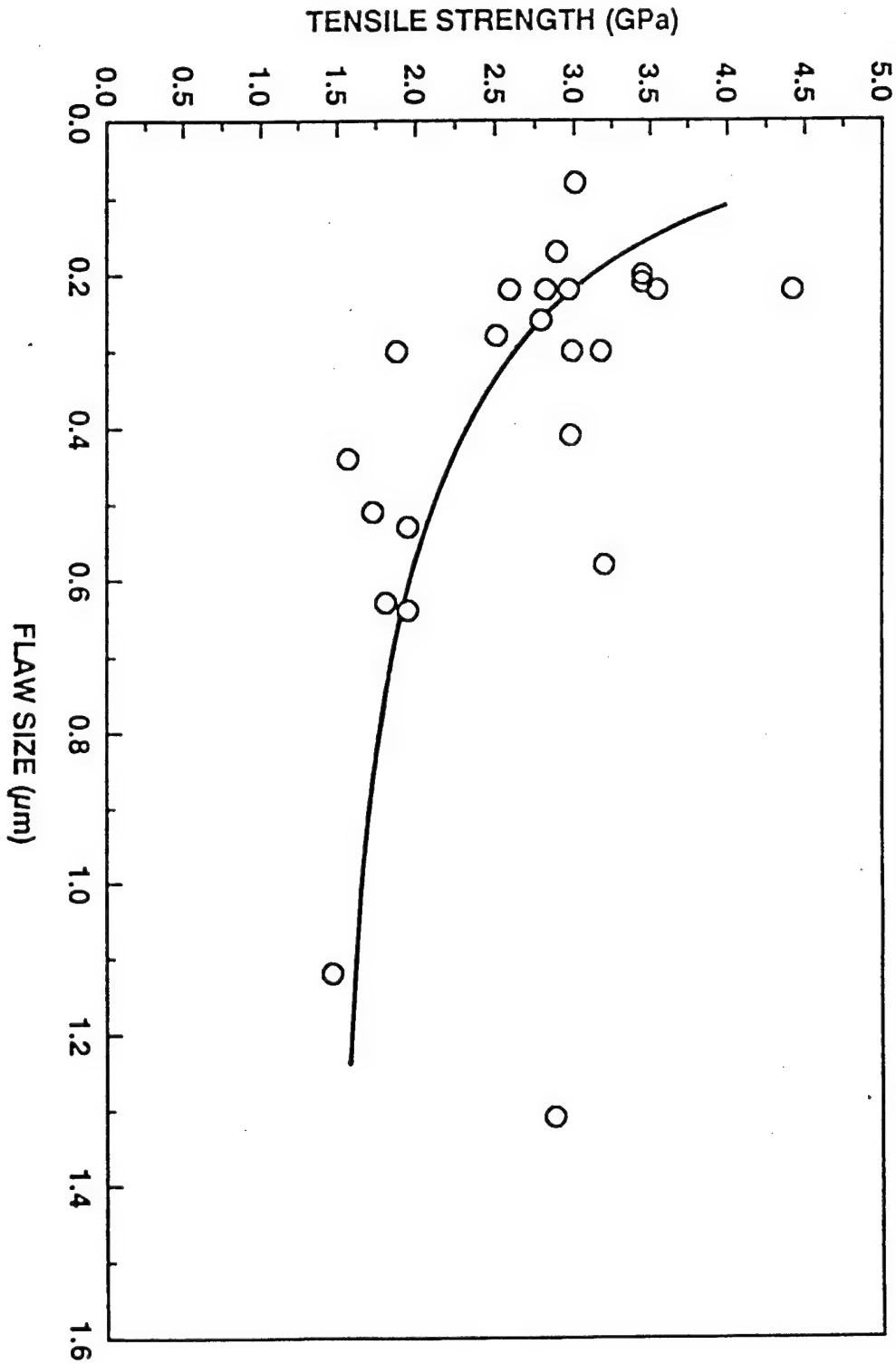
TENSILE STRENGTH (GPa)
0.0
0.5
1.0
1.5
2.0
2.5
3.0
3.5
4.0
4.5
5.0
FLAW SIZE (μm)
0.0
0.2
0.4
0.6
0.8
1.0
1.2
1.4
1.6

Figure 3

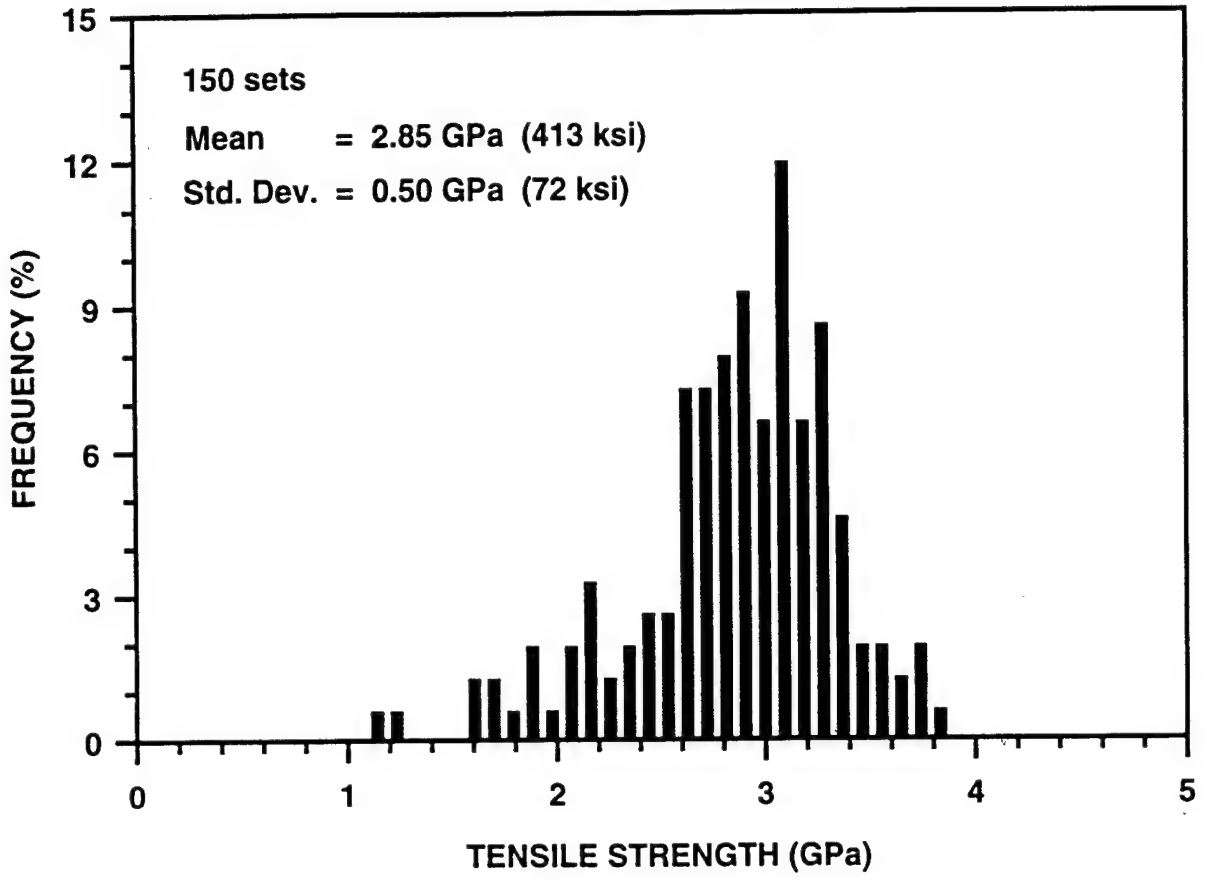
150 sets
Mean = 2.85 GPa (413 ksi)
Std. Dev. = 0.50 GPa (72 ksi)
FREQUENCY (%)
TENSILE STRENGTH (GPa)
0
3
6
9
12
15
0
1
2
3
4
5

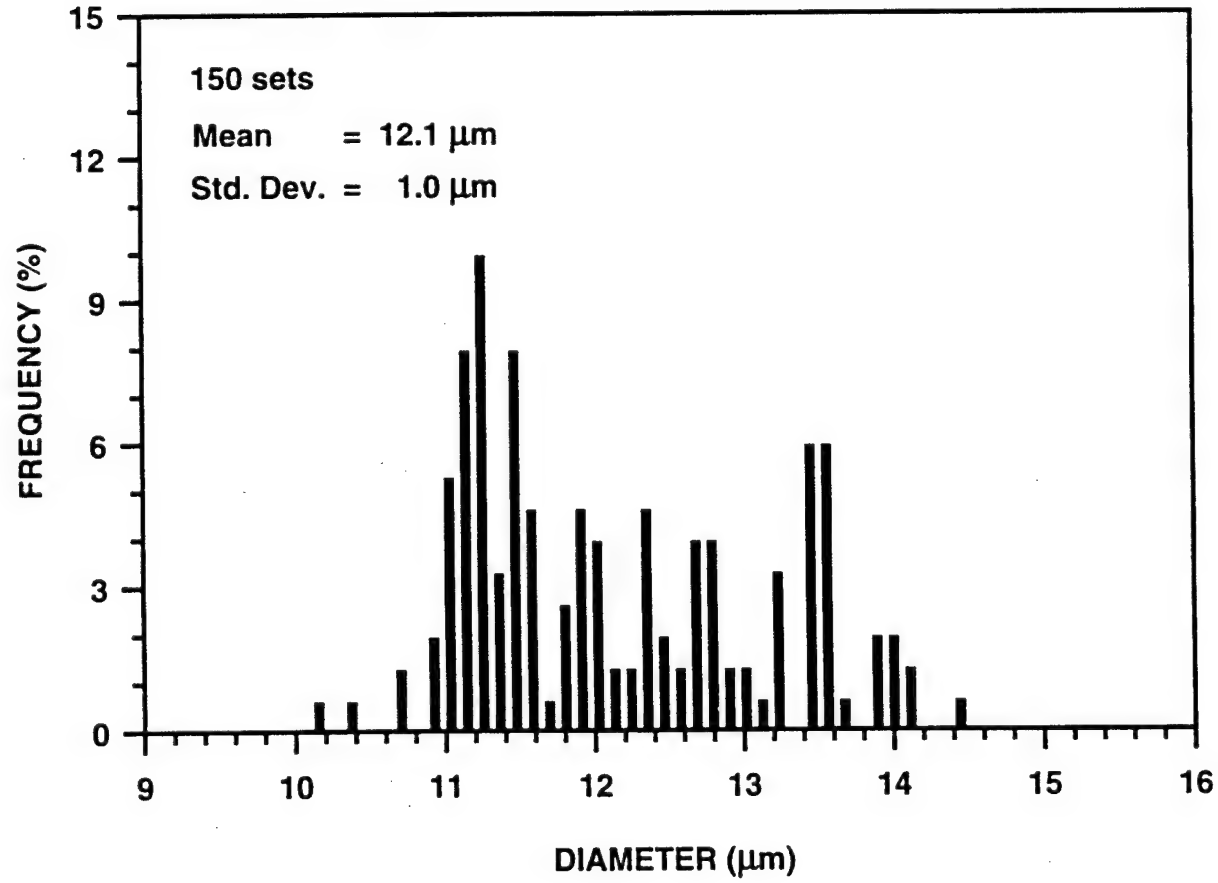
150 sets
Mean = 12.1 µm
Std. Dev. = 1.0 µm
FREQUENCY (%)
DIAMETER (µm)
0
3
6
9
12
15
9
10
11
12
13
14
15
16

Figure 4

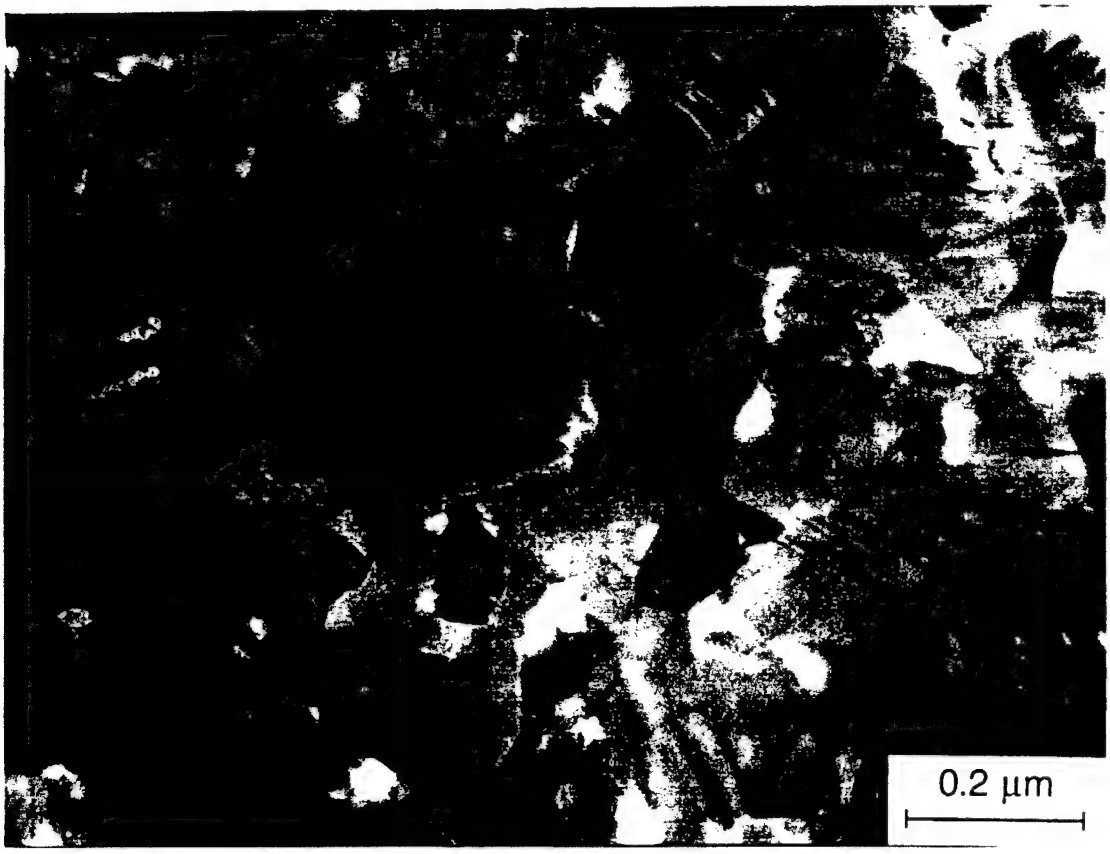

Figure 5

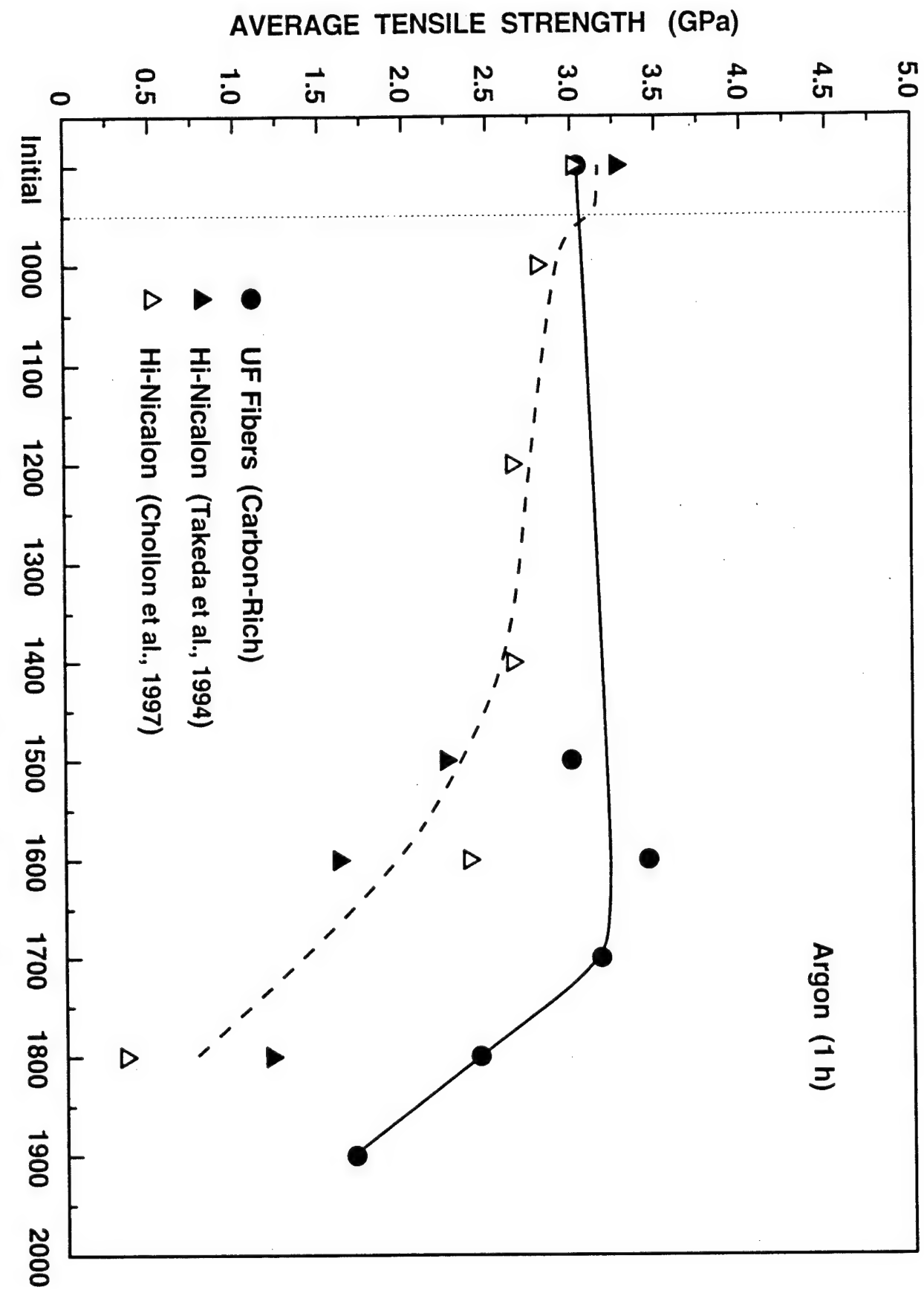
AVERAGE TENSILE STRENGTH (GPa)
0
0.5
1.0
1.5
2.0
2.5
3.0
3.5
4.0
4.5
5.0
Initial
1000
1100
1200
1300
1400
1500
1600
1700
1800
1900
2000
HEAT TREATMENT TEMPERATURE (°C)
Argon (1 h)
UF Fibers (Carbon-Rich)
Hi-Nicalon (Takeda et al., 1994)
Hi-Nicalon (Chollon et al., 1997)

Figure 6

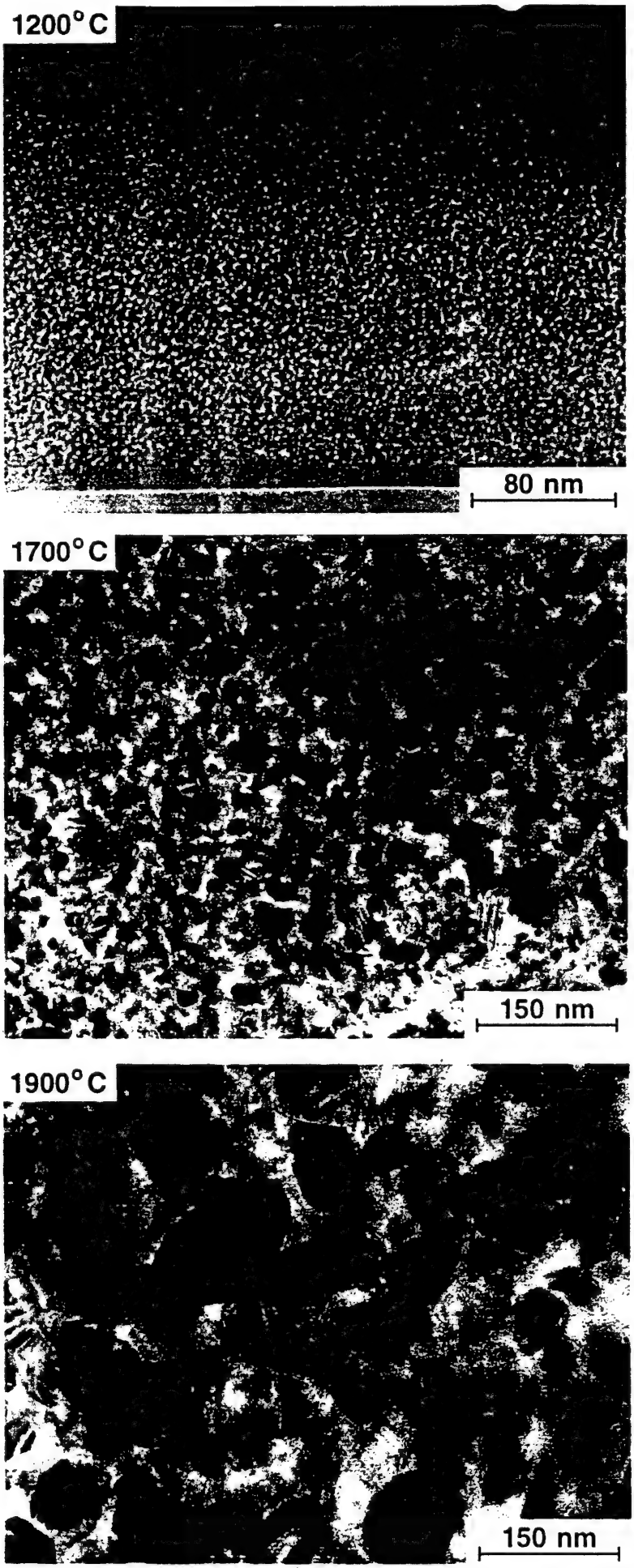

Figure 7

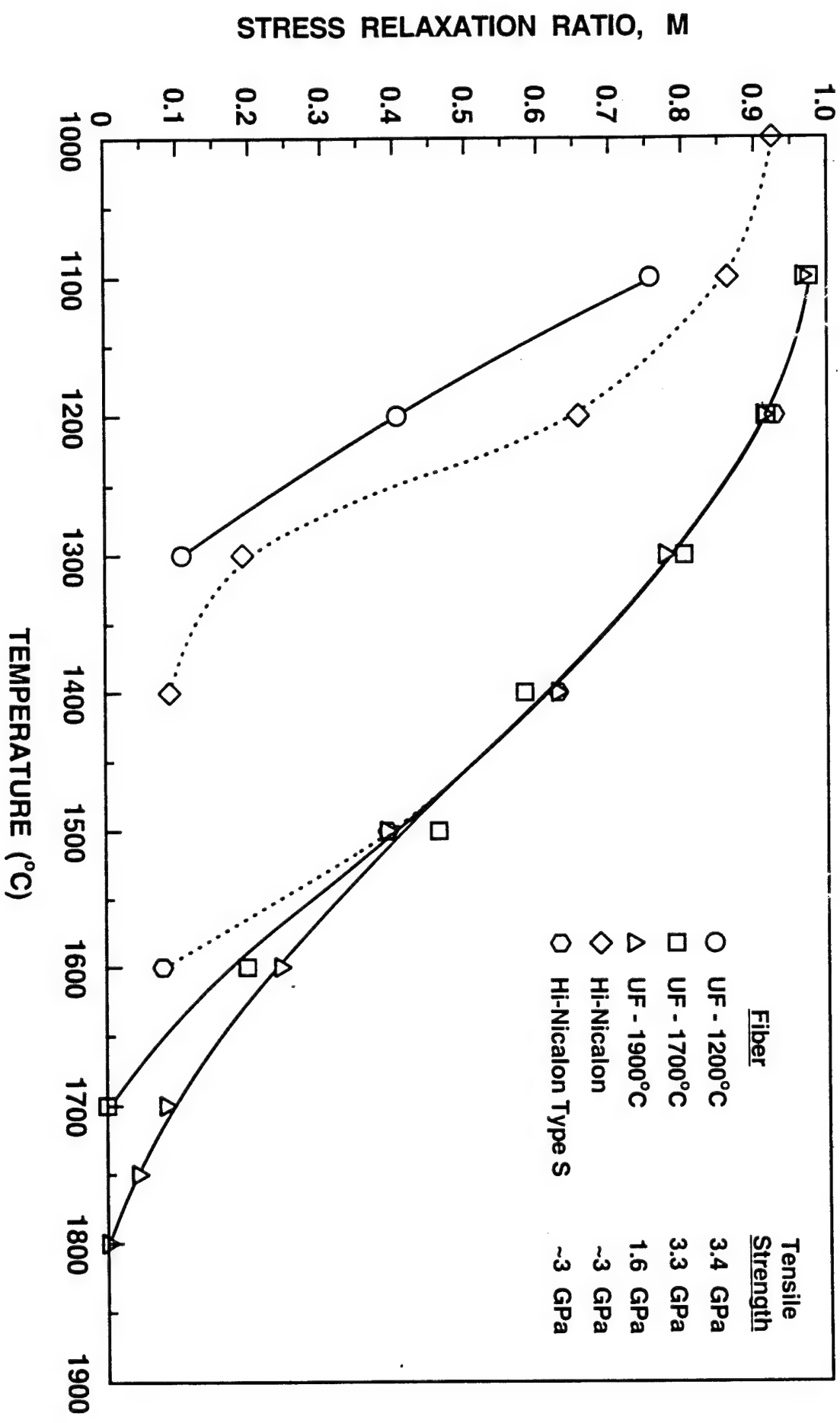
STRESS RELAXATION RATIO, M
1.0
0.9
0.8
0.7
0.6
0.5
0.4
0.3
0.2
0.1
0
1000
1100
1200
1300
1400
1500
1600
1700
1800
1900
TEMPERATURE (°C)
Fiber
Tensile Strength
UF - 1200°C 3.4 GPa
UF - 1700°C 3.3 GPa
UF - 1900°C 1.6 GPa
Hi-Nicalon ~3 GPa
Hi-Nicalon Type S ~3 GPa

Figure 8

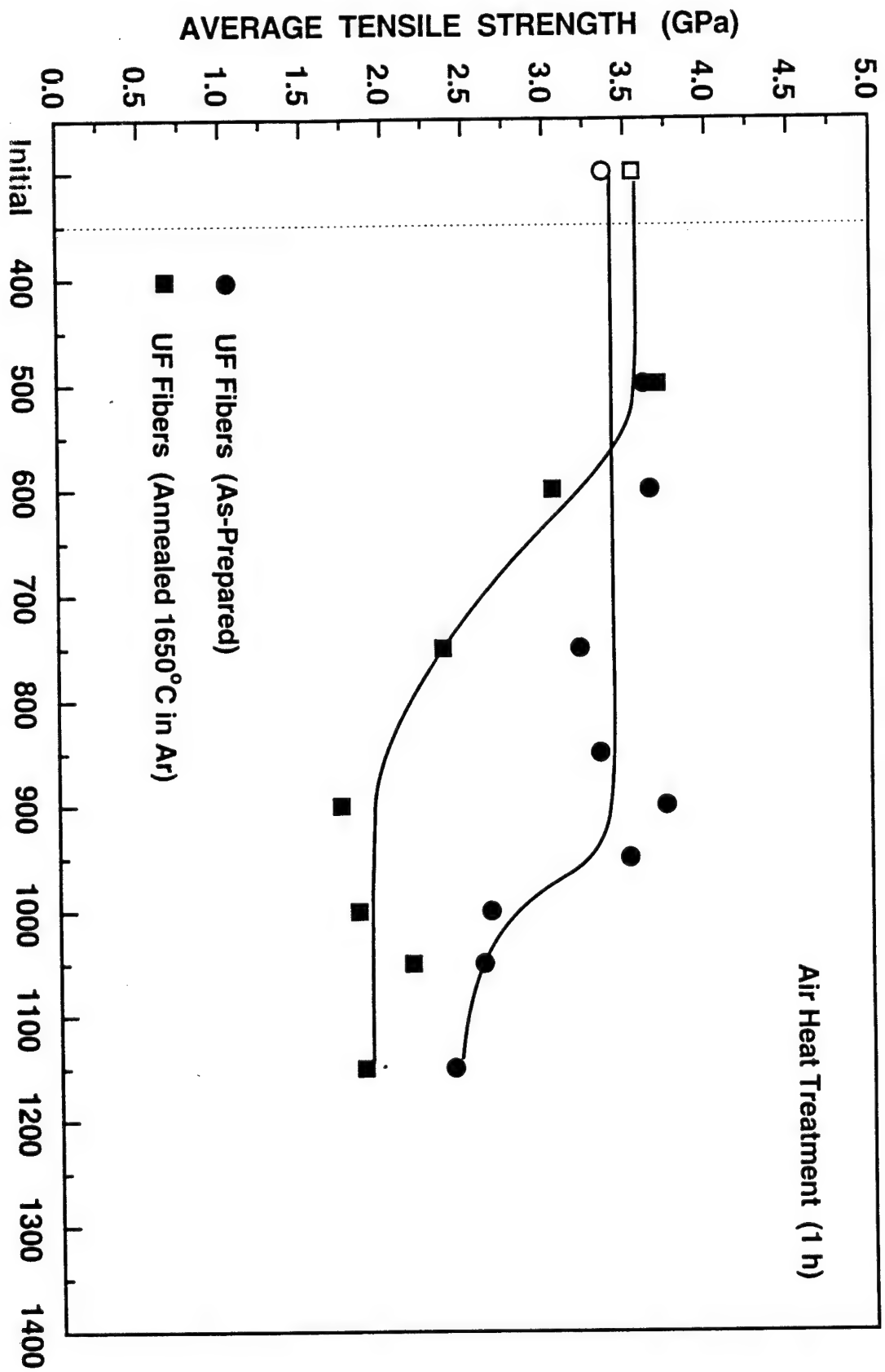
AVERAGE TENSILE STRENGTH (GPa)
5.0
4.5
4.0
3.5
3.0
2.5
2.0
1.5
1.0
0.5
0.0
Air Heat Treatment (1 h)
UF Fibers (As-Prepared)
UF Fibers (Annealed 1650°C in Ar)
Initial
400
500
600
700
800
900
1000
1100
1200
1300
1400
HEAT TREATMENT TEMPERATURE (°C)

Figure 9

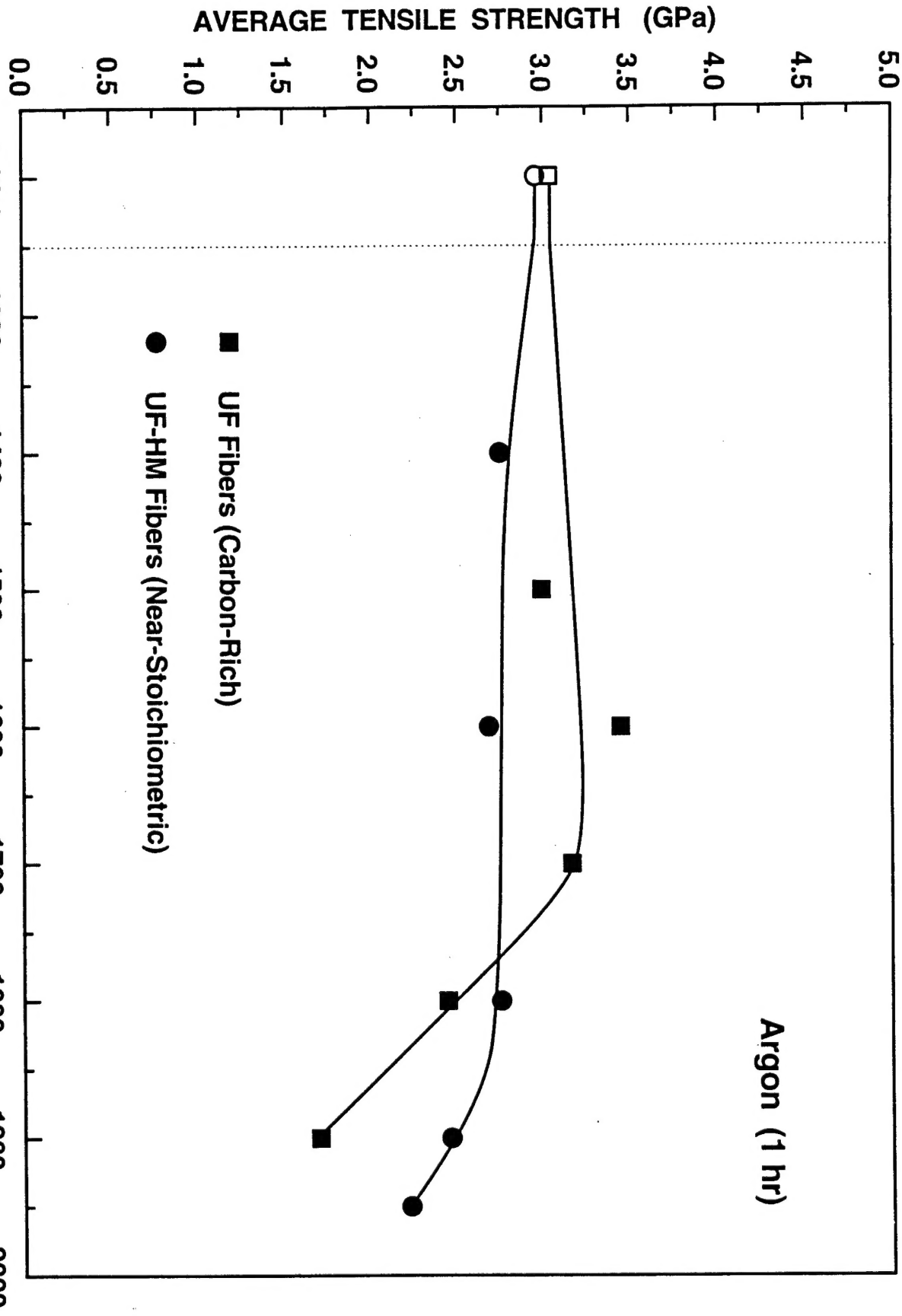
AVERAGE TENSILE STRENGTH (GPa)
0.0
0.5
1.0
1.5
2.0
2.5
3.0
3.5
4.0
4.5
5.0
Initial
1300
1400
1500
1600
1700
1800
1900
2000
HEAT TREATMENT TEMPERATURE (°C)
UF Fibers (Carbon-Rich)
UF-HM Fibers (Near-Stoichiometric)
Argon (1 hr)

Figure 10

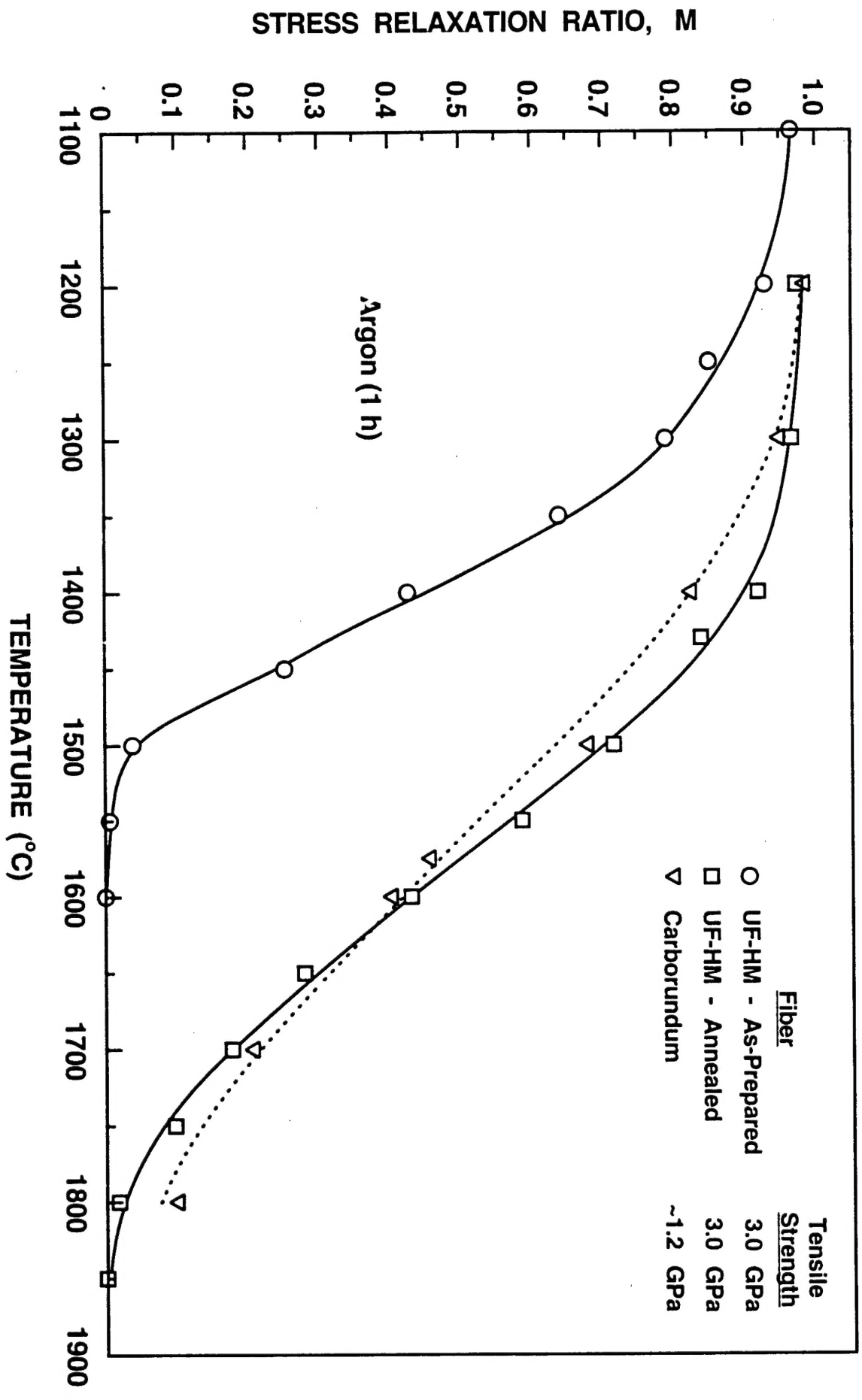
STRESS RELAXATION RATIO, M
1.0
0.9
0.8
0.7
0.6
0.5
0.4
0.3
0.2
0.1
0
1100
1200
1300
1400
1500
1600
1700
1800
1900
TEMPERATURE (°C)
Argon (1 h)
Fiber
Tensile Strength
UF-HM - As-Prepared 3.0 GPa
UF-HM - Annealed 3.0 GPa
Carborundum ~1.2 GPa

Figure 11

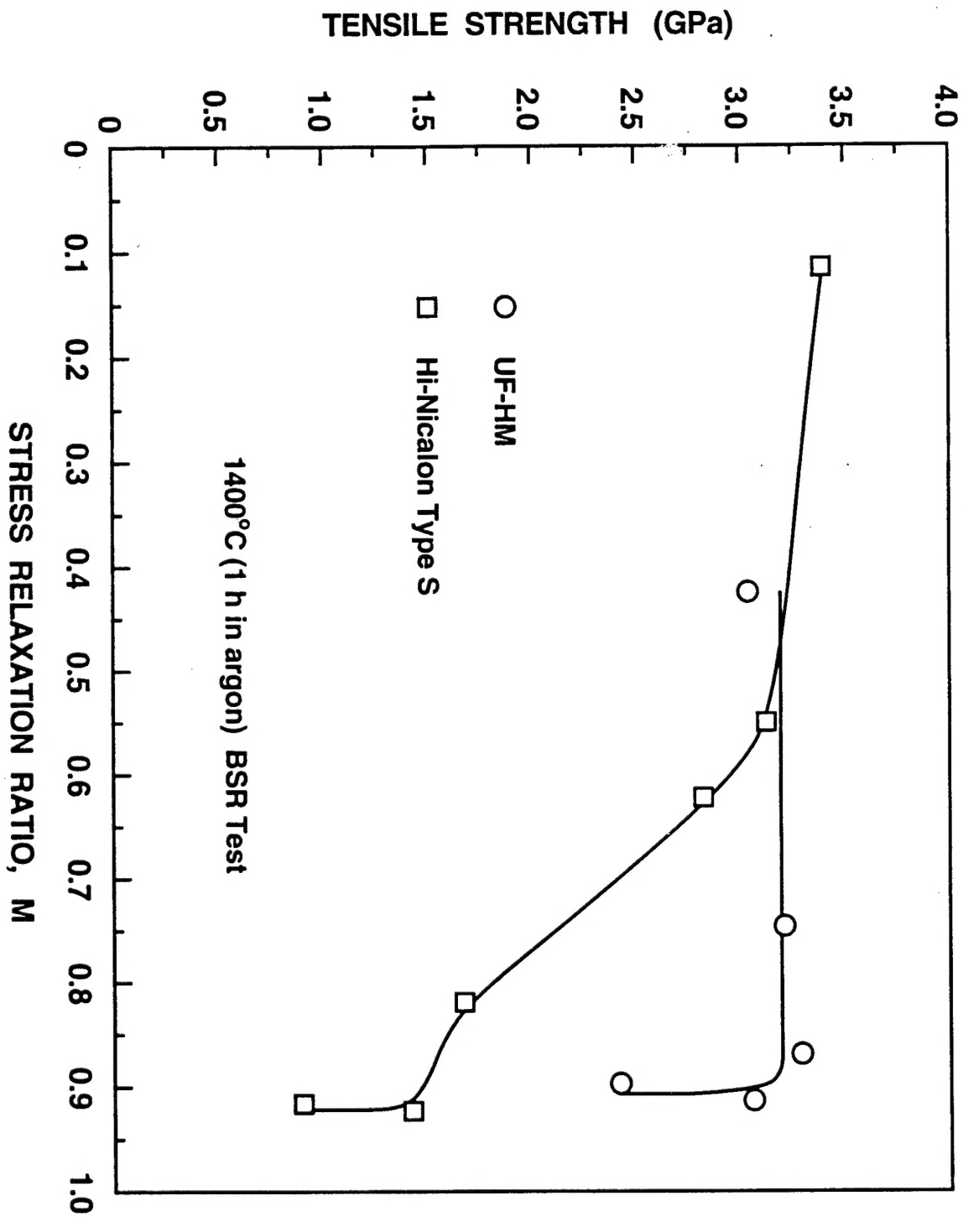
TENSILE STRENGTH (GPa)
0
0.5
1.0
1.5
2.0
2.5
3.0
3.5
4.0
0
0.1
0.2
0.3
0.4
0.5
0.6
0.7
0.8
0.9
1.0
STRESS RELAXATION RATIO, M
Hi-Nicalon Type S
UF-HM
1400°C (1 h in argon) BSR Test

Figure 12

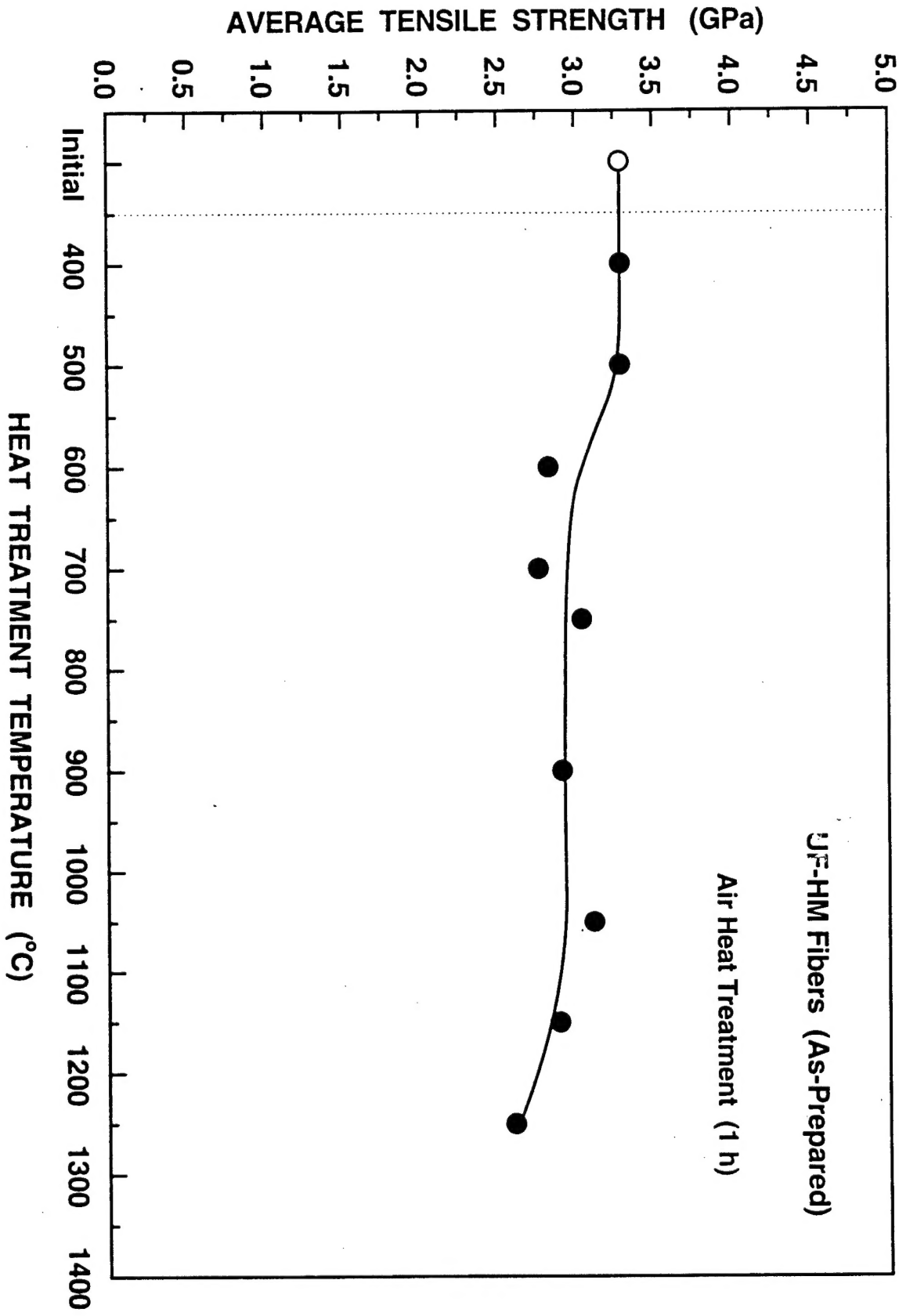
AVERAGE TENSILE STRENGTH (GPa)
0.0
0.5
1.0
1.5
2.0
2.5
3.0
3.5
4.0
4.5
5.0
Initial
400
500
600
700
800
900
1000
1100
1200
1300
1400
HEAT TREATMENT TEMPERATURE (°C)
UF-HM Fibers (As-Prepared)
Air Heat Treatment (1 h)